

# Estimation of Population Size with Heterogeneous Catchability and Behavioural Dependence: Applications to Air and Water Borne Disease Surveillance

Prajamitra Bhuyan<sup>†</sup> Kiranmoy Chatterjee\* <sup>1</sup>

<sup>†</sup>Indian Institute of Management, Calcutta

\*Bidhannagar College Kolkata

## Abstract

Population size estimation based on the capture-recapture experiment is an interesting problem in various fields including epidemiology, criminology, demography, etc. In many real-life scenarios, there exists inherent heterogeneity among the individuals and dependency between capture and recapture attempts. A novel trivariate Bernoulli model is considered to incorporate these features, and the Bayesian estimation of the model parameters is suggested using data augmentation. Simulation results show robustness under model misspecification and the superiority of the performance of the proposed method over existing competitors. The method is applied to analyse real case studies on epidemiological surveillance. The results provide interesting insight on the heterogeneity and dependence involved in the capture-recapture mechanism. The methodology proposed can assist in effective decision-making and policy formulation.

*Key words:* COVID-19, Gibbs sampling, Hepatitis A, List dependence, Multiple systems estimation.

## 1 Introduction

The knowledge about the true prevalence of a disease in a specified period is an essential requirement for surveillance and effective policy formulation regarding the healthcare system of a state (Bird and King, 2018). In general, the available data source fails to cover all the relevant events and that leads to an undercount of the target population suffering from the disease. Therefore, disease ascertainment data are accumulated from multiple sources to increase the

---

<sup>1</sup>Both authors contributed equally to this paper.

coverage and for the estimation of the disease prevalence (Papoz et al., 1996). This method is known as multiple system estimation (MSE) which is equivalent to the capture-mark-recapture (CMR) method traditionally applied to estimate the size of wildlife populations (Hook and Regal, 1995; International Working Group for Disease Monitoring and Forecasting, 1995). The MSE is also popularly used for the estimation of demographic counts such as births and deaths (O’Hara et al., 2009), census undercoverage (Zaslavsky and Wolfgang, 1993), crime incidence (Cruyff et al., 2017), number of beneficiaries in a welfare economic study (Bird and King, 2018), etc. Lately, the MSE is also applied in clinical settings for screening and preventive studies (Bohning and Heijden, 2009).

The MSE involves the matching of the individuals enlisted from different sources and recording the various forms of overlaps among these lists. Traditionally two sources are considered, and it is a common practice to assume the independence between the lists for the estimation of population size which in many cases is affected by the correlation bias when the underlying assumption fails (ChandraSekar and Deming, 1949). In most cases, these sources of information are dependent because an individual’s behaviour changes with the time of subsequent recapture attempts after the initial attempt. Another possible reason for dependence between lists is that capture probability may vary across individuals in each list (Chao et al., 2001). Therefore, more than two data sources are considered to capture more eligible events and to assess the underlying interdependence among the lists. In particular, three samples or lists are commonly considered in epidemiological surveillance (Gallay et al., 2000; Van Hest, 2007; Ruche et al., 2013). Note that the population of interest is assumed closed during the ascertainment of events from the three sources which generally occurs within a short period. The data obtained from three different sources are summarized in the form of an incomplete  $2^3$  contingency table. This data structure, presented in Table S1 of the Supplementary Material, is typically known as the triple record system (TRS). Denote the capture status of an event in the first, second, and third lists by  $i$ ,  $j$ , and  $k$ , respectively. The dummy variables  $i$ ,  $j$ , and  $k$  take value 1 for capture and 0 otherwise. The total number of events with a particular capture status, say  $(i, j, k)$ , is denoted by  $x_{ijk}$ . For example, the count  $x_{101}$  associated with the cell  $(1, 0, 1)$  represents the number of events that appear in the first and the third lists but are absent in the second list. Note that  $N = \sum_{i,j,k} x_{ijk} = n + x_{000}$ , where  $n = \sum_{i,j,k \neq 0} x_{ijk}$  refers to the total number of individuals that are recorded at least in one list, and  $x_{000}$  refers the total count of individuals that are not recorded in any of the three lists. Therefore, the

problem of estimating the population size  $N = \sum_{i,j,k} x_{ijk}$  is equivalent to that of the unknown cell count  $x_{000}$ . Interested readers are referred to [Zaslavsky and Wolfgang \(1993\)](#); [Chatterjee and Bhuyan \(2020b\)](#) for a detailed discussion on TRS and associated estimation methodology. In this article, we consider the problem of estimating disease prevalence motivated by TRS data available from the following case studies on epidemiological surveillance related to fatal illness due to air and water borne bacteria and viruses.

## 1.1 Legionnaires' Disease

Legionnaires' Disease (LD) is an unusual variant of pneumonia that occurs sporadically and in outbreaks caused by the bacterium Legionella which spreads through airborne water droplets ([Den et al., 2002b](#); [Lettinga et al., 2002](#)). The motivation for considering surveillance on LD is two-fold in light of the current pandemic of COVID-19. Firstly, reports of co-infection with respiratory pathogens are increasing throughout the world ([Lai et al., 2020](#)). It has also been reported that 50% of COVID-19 patients who succumbed had secondary bacterial infections like LD ([Zhou et al., 2020](#)). Secondly, patients with COVID-19 should be screened for LD because the signs and symptoms of both infections are similar. The scientific community very recently found that COVID-19 infections can predispose patients to Legionella co-infections and consequently pose a serious threat to high-risk COVID-19 patients, which can lead to an increase in the severity of LD and mortality ([Dey and Ashbolt, 2020](#)).

The Netherlands is one of the worst affected countries by LD in the world. We consider a study on LD in the Netherlands conducted during the period from 2000 to 2001 ([Van Hest et al., 2008](#)). The average national annual prevalence rate of LD was 1.4 patients per 100 thousand inhabitants of the Netherlands in 1999. But experts suspect that the conventional LD notification system contains false-positive cases and is often incomplete for true positive cases of LD ([Van Hest et al., 2008](#)). In this regard, efficient record-linkage and capture-recapture analysis for assessing the quality and completeness of infectious disease registers are warranted. In this study, information on LD-affected patients is collected from Disease Notifications Register (DNR) from the Health Care Inspectorate, Laboratory results, and Hospital admissions. In the DNR, 373 LD patients are identified through record linkage. On the other hand, a total of 261 patients with a positive test for LD are recorded from the Laboratory survey. In total, 663 patients are enlisted in the hospital records with a relatively

large number of 332 patients captured exclusively in this list. The overlap counts associated with these three lists are provided in Section 1 of the Supplementary Material (see Table S2). The presence of dominant interaction between the DNR and the Laboratory register has been indicated in a previous study (Van Hest et al., 2008). Moreover, various factors like geographical region, age, and laboratory diagnostics technique cause heterogeneity in the capture probabilities of the individuals in each list (Nardone et al., 2003; Den et al., 2002a).

## 1.2 Hepatitis A Virus

Viral hepatitis is among the top ten leading causes of mortality worldwide and is the only communicable disease where mortality is increasing (Brown et al., 2017). The hepatitis A virus (HAV) spreads through person-to-person contact and contaminated food or water. In high-income countries, HAV infection usually occurs among drug addicts, and men having sex with men, including patients with HIV and other sexually transmitted infections due to a low prevalence of anti-HAV antibodies (Cuthbert, 2001; Chen et al., 2019). The scientific community opines that continuous HAV surveillance and evaluation of long-term vaccine effectiveness among HIV patients are warranted and HAV vaccination for all in childhood will provide more sustainable immunity in the general population. Therefore, it is important to know the actual population size infected with HAV for efficient vaccination policy and disease surveillance.

Approximately 1.4 million infections are reported worldwide each year, of which approximately half occur in Asian countries (Martin and Lemon, 2006). In particular, Taiwan has a history of a high prevalence of HAV infection because of indigenous townships with inadequate water, sanitation, and hygiene infrastructure in the last decade of the twentieth century (Chen et al., 2019). We consider a study on HAV outbreak in northern Taiwan from April to July 1995 near a technical college (Chao et al., 1997). There are three registered sources of information on the HAV infected college students available: (i) P-list consists of 135 records based on a serum test taken by the Institute of Preventive Medicine, Department of Health of Taiwan, (ii) Q-list includes 122 cases reported by doctors in local hospitals and this list was provided by the National Quarantine Service and (iii) E-list comprise of 126 cases based on questionnaires conducted by epidemiologists. Tsay and Chao (2001) reported the existence of heterogeneity in capture probabilities in all three sources, and low overlap has been observed among the lists. The summarized data are provided in Table S2 in Section 1 of the Supplementary Material.

### 1.3 The Challenges in Analysing TRS Data

As mentioned before, the assumption of list independence is often violated in practice mainly due to two reasons: (i) list dependence caused by behavioural response variation over different sources, i.e. the inclusion status of an individual in one list has a direct causal effect on his/her inclusion status in other lists; (ii) heterogeneity in the propensity to be captured in a list over individuals (Chao et al., 2001). Even when no behavioural response variation occurs for individuals over different lists, their ascertainment in the lists becomes positively dependent if the capture probabilities are heterogeneous across individuals in each list (ChandraSekar and Deming, 1949; Chao, 2015). We call this second type of list dependence as heterogeneity-induced list dependence (Darroch et al., 1993). In both the case studies, discussed in sections 1.1 and 1.2, the associated TRS datasets are potentially affected by the list dependence because of these two aforementioned reasons.

In the literature of MSE for closed population, various models account for the first kind of list dependence i.e. dependence due to the behavioural change in response of each individual at the time of subsequent attempts after the first capture. This is called behavioural list dependence. Fienberg (1972) proposed a log-linear model (LLM) incorporating various possible interactions among the available lists. An overview of the LLMs and their applications for population size estimation are provided in Cormack (1989); International Working Group for Disease Monitoring and Forecasting (1995). However, the parameters associated with the LLMs are not well interpretable to the practitioners (Coumans et al., 2017). In this context, model  $M_{tb}$  is frequently used in ecological surveillance to account for the list dependence due to behavioural response variation (Otis et al., 1978). This model may produce unstable estimates in many instances (Rivest and Baillargion, 2022) and has several other limitations in the context of human population (Chatterjee and Bhuyan, 2020a). To model the individual heterogeneity, Sanathanan (1972b) adapted the Rasch model and derived associated estimation methodology. Later, Goodman (1974) developed latent class models assuming the population is composed of homogeneous strata with independent lists. Darroch et al. (1993) provided some variants of the heterogeneity model by extending the log-linear representation of the Rasch model, such as quasi-symmetry and partial quasi-symmetry models (Chao and Tsay, 1998). However, model selection in the case of LLMs may be difficult because an adequate fit to the observed cells may not necessarily produce an efficient estimate of the unobserved

cell (Chao, 2015). Also, the existence of heterogeneity in data might result in the lack of a reliable estimate (International Working Group for Disease Monitoring and Forecasting, 1995). Recently, Manrique-Vallier (2016a) developed a Bayesian non-parametric method to accommodate individual heterogeneity based on Dirichlet process mixtures assuming independence between the lists.

The most general scenario of the capture-recapture experiment encompasses both the list dependence due to behavioural response variation and individual heterogeneity in the capture probabilities of the individuals. The heterogeneity-induced dependence among lists is generally confounded with the list dependence due to behavioural response variation (Chao, 2001). Such a complex scenario may often arise in various fields of applications including epidemiology (Tsay and Chao, 2001; Van Hest et al., 2008). It is challenging to incorporate these two factors together in a model and provide an efficient estimate of the population size for TRS data (Chao et al., 2001). In this context, an ecological model  $M_{bh}$  has been developed to estimate the abundance of the animal population (Otis et al., 1978). However, the reliability of the estimate based on this model depends on several conditions, including the sequential ordering of the capture sampling (Otis et al., 1978). These conditions may not be relevant for MSE. As a result, this model may produce an inefficient and/or infeasible estimate (see Sections 4-5). Chao's non-parametric sample coverage approach accounts for both the individual heterogeneity and possible interaction between the lists (Chao and Tsay, 1998; Chao, 2015). However, the performance of this estimator is not satisfactory as it may also provide infeasible estimates. See Section 4 for details.

In this article, we propose a novel modeling approach based on the trivariate Bernoulli model that incorporates both the behavioural dependence between the lists and the individual heterogeneity along with the list variation. The parameters of the model are easily interpretable and provide interesting insights into the capture-recapture mechanism. We develop a Bayesian estimation methodology for the estimation of  $N$  and associated model parameters. In particular, we demonstrate how Gibbs sampling facilitates Bayesian analysis of capture-recapture experiments in the most general as well as complex scenarios. As a result, formulations that were previously avoided because of analytical intractability and computational time can now be easily considered for practical applications. The description of the proposed model and its special cases are provided in Section 2. In Section 3, estimation methodologies for the population size  $N$  and associated model parameters are discussed. Next, the performance of the

proposed method is compared with the existing competitors through an extensive simulation in Section 4. Sensitivity analyses concerning prior choices and model mis-specifications are also discussed in the same section. Analyses of the real datasets on LD and HAV are presented in Section 5. We summarise the key findings and conclude with some discussion on future research in Section 6.

## 2 Modeling Individual Heterogeneity and List Dependence

In this section, we first discuss the Trivariate Bernoulli model (TBM) proposed by [Chatterjee and Bhuyan \(2020a\)](#) for modeling capture–recapture data under TRS. The TBM is used to incorporate the inherent list dependence, and its parameters possess physical interpretation. We extend this model in a more general setup to account for the ‘individual heterogeneity’ in addition to the list dependence.

In TRS, some individuals behave independently over the three different capture attempts and behavioural dependence exists for the rest of the population. To model the association among the three lists  $L_1$ ,  $L_2$  and  $L_3$ , we first consider that  $\alpha_1$ ,  $\alpha_2$ , and  $\alpha_3$  proportion of individuals possess pairwise dependence between lists ( $L_1$  and  $L_2$ ), ( $L_2$  and  $L_3$ ) and ( $L_1$  and  $L_3$ ). Further, we consider the second-order dependency among the three lists  $L_1$ ,  $L_2$ , and  $L_3$  for  $\alpha_4$  proportion of individuals. Therefore, the remaining  $(1 - \alpha_0)$  proportion of individuals, where  $\alpha_0 = \sum_{\omega=1}^4 \alpha_{\omega}$ , behave independently over the three lists. Now we define a triplet  $(X_{1h}^*, X_{2h}^*, X_{3h}^*)$  which represents the latent capture statuses of the  $h$ th individual in the first, second and third attempts respectively, for  $h = 1, 2, \dots, N$ . The latent capture status  $X_{sh}^*$  takes the value 1 or 0, denoting the presence or absence of the  $h$ th individual in the  $s$ th list, for  $s = 1, 2, 3$ . Under this setup,  $X_{2h}^* = X_{1h}^*$  and  $X_{3h}^* = X_{2h}^*$  for  $\alpha_1$  and  $\alpha_2$  proportion of individuals, respectively. Similarly,  $X_{3h}^* = X_{1h}^*$  for  $\alpha_3$  proportion of individuals, and  $X_{3h}^* = X_{2h}^* = X_{1h}^*$  for  $\alpha_4$  proportion of individuals. Now, denote  $Z_h^{(1)}$ ,  $Z_h^{(2)}$ , and  $Z_h^{(3)}$  as the the inclusion statuses of the  $h$ th individual in  $L_1$ ,  $L_2$ , and  $L_3$  respectively, for  $h = 1, 2, \dots, N$ . Therefore, we can

formally write the model to account for the interdependence among the three lists as:

$$(Z_h^{(1)}, Z_h^{(2)}, Z_h^{(3)}) = \begin{cases} (X_{1h}^*, X_{1h}^*, X_{3h}^*) & \text{with prob. } \alpha_1, \\ (X_{1h}^*, X_{2h}^*, X_{2h}^*) & \text{with prob. } \alpha_2, \\ (X_{1h}^*, X_{2h}^*, X_{1h}^*) & \text{with prob. } \alpha_3, \\ (X_{1h}^*, X_{1h}^*, X_{1h}^*) & \text{with prob. } \alpha_4, \\ (X_{1h}^*, X_{2h}^*, X_{3h}^*) & \text{with prob. } 1 - \alpha_0, \end{cases} \quad (1)$$

where  $X_{1h}^*$ 's,  $X_{2h}^*$ 's and  $X_{3h}^*$ 's are independently distributed Bernoulli random variables with parameters  $\mathcal{P}_1$ ,  $\mathcal{P}_2$  and  $\mathcal{P}_3$ , respectively, for all  $h = 1, \dots, N$ . Note that  $\mathcal{P}_s$  refers to the capture probability of a causally independent individual in the  $s$ th list. To incorporate heterogeneity in capture probabilities, we now consider  $X_{1h}^*$ 's to follow independent Bernoulli distributions with parameter  $\mathcal{P}_{sh}$  and model it as:

$$\text{logit}(\mathcal{P}_{sh}) = \log \left( \frac{\mathcal{P}_{sh}}{1 - \mathcal{P}_{sh}} \right) = b_{sh}, \quad h = 1, \dots, N, \quad (2)$$

where  $b_{sh}$ 's are independent and identically distributed realizations of random effect  $b_s$ , for each  $s = 1, 2, 3$ . We also assume  $b_s$ 's are independently distributed. We refer to this generic model, given in (1) and (2), as the Trivariate Heterogeneous Bernoulli model (THBM).

## 2.1 Special Cases

The generic form of the proposed THBM incorporates the list variation, individual heterogeneity, and behavioural dependence arising from different sources. However, in some cases, the effect of the behavioural response variation is confounded due to heterogeneous catchability and may not provide additional information for the estimation of  $N$ . In such cases, it is prudent to consider a parsimonious model with some restrictions on the THBM. In particular, one can consider  $\alpha_\omega = 0$ , for  $\omega = 1, \dots, 4$ , and this reduced model is applicable for the scenarios where the generalized Rasch model is useful (Darroch et al., 1993; Chao and Tsay, 1998) (see Section 2.2 of the Supplementary Material). One can further assume  $b_l$ 's are identically distributed where the catchability is the same over the individuals irrespective of the lists. The THBM model reduces to TBM when  $b_l$ 's are degenerate random variables. This model is useful for TRS when the individuals are equally catchable in each list. As discussed in Chatterjee and

[Bhuyan \(2020a\)](#), the TBM can be further reduced to the submodels TBM-1 and TBM-2 if we consider  $\alpha_3 = 0$  and  $\alpha_4 = 0$ , respectively. In the absence of list dependence (i.e.  $\alpha_\omega = 0$ , for  $\omega = 1, \dots, 4$ ) the TBM and the  $M_t$  model are equivalent ([Otis et al., 1978](#)).

### 3 Estimation Methodology

A classical approach for estimating  $N$  in the context of CMR is based on the likelihood theory, where the vector of observed cell counts

$$\mathbf{x} = \left\{ x_{ijk} : x_{ijk} = \sum_{h=1}^n \mathbb{I} \left[ Z_h^{(1)} = i, Z_h^{(2)} = j, Z_h^{(3)} = k \right]; i, j, k = 0, 1; i = j = k \neq 0 \right\}$$

(as presented in Table S1 of the Supplementary Material, follow a multinomial distribution with index parameter  $N$  and the associated cell probabilities  $\mathbf{p} = \{p_{ijk} : i, j, k = 0, 1; i = j = k \neq 0\}$  ([Sanathanan, 1972a](#)), where  $\mathbb{I}[\cdot]$  denotes indicator function. Therefore, the likelihood function is given by

$$L(N, \mathbf{p} | \mathbf{x}) = \frac{N!}{\prod_{i,j,k=0,1; i=j=k \neq 0} x_{ijk}!(N-n)!} \prod_{i,j,k=0,1} p_{ijk}^{x_{ijk}},$$

where  $x_{000} = N - n$ . The TBM is characterized by the parameters  $N$ ,  $\alpha_1$ ,  $\alpha_2$ ,  $\alpha_3$ ,  $\alpha_4$ ,  $\mathcal{P}_1$ ,  $\mathcal{P}_2$ ,  $\mathcal{P}_3$ , and using its relationships with the cell probabilities  $p_{ijk}$ , the likelihood function is given by

$$\begin{aligned} L(N, \boldsymbol{\alpha}, \mathbf{P} | \mathbf{x}) \propto & \frac{N!}{(N-n)!} [(1 - \alpha_0)\mathcal{P}_1\mathcal{P}_2\mathcal{P}_3 + \alpha_1\mathcal{P}_1\mathcal{P}_3 + \alpha_2\mathcal{P}_1\mathcal{P}_2 + \alpha_3\mathcal{P}_1\mathcal{P}_2 + \alpha_4\mathcal{P}_1]^{x_{111}} \\ & \times [(1 - \alpha_0)\mathcal{P}_1\mathcal{P}_2(1 - \mathcal{P}_3) + \alpha_1\mathcal{P}_1(1 - \mathcal{P}_3)]^{x_{110}} \\ & \times [(1 - \alpha_0)(1 - \mathcal{P}_1)\mathcal{P}_2\mathcal{P}_3 + \alpha_2(1 - \mathcal{P}_1)\mathcal{P}_2]^{x_{011}} \\ & \times [(1 - \alpha_0)\mathcal{P}_1(1 - \mathcal{P}_2)(1 - \mathcal{P}_3) + \alpha_2\mathcal{P}_1(1 - \mathcal{P}_2)]^{x_{100}} \\ & \times [(1 - \alpha_0)\mathcal{P}_1(1 - \mathcal{P}_2)\mathcal{P}_3 + \alpha_3\mathcal{P}_1(1 - \mathcal{P}_2)]^{x_{101}} \\ & \times [(1 - \alpha_0)(1 - \mathcal{P}_1)\mathcal{P}_2(1 - \mathcal{P}_3) + \alpha_3(1 - \mathcal{P}_1)\mathcal{P}_2]^{x_{010}} \\ & \times [(1 - \alpha_0)(1 - \mathcal{P}_1)(1 - \mathcal{P}_2)\mathcal{P}_3 + \alpha_1(1 - \mathcal{P}_1)\mathcal{P}_3]^{x_{001}} \\ & \times [(1 - \alpha_0)(1 - \mathcal{P}_1)(1 - \mathcal{P}_2)(1 - \mathcal{P}_3) + \alpha_1(1 - \mathcal{P}_1)(1 - \mathcal{P}_3) \\ & + \alpha_2(1 - \mathcal{P}_1)(1 - \mathcal{P}_2) + \alpha_3(1 - \mathcal{P}_1)(1 - \mathcal{P}_2) + \alpha_4(1 - \mathcal{P}_1)]^{N-n}, \end{aligned} \quad (3)$$

where  $p_{000} = 1 - \sum_{i,j,k=0,1; i=j=k \neq 0} p_{ijk}$ ,  $\boldsymbol{\alpha} = (\alpha_1, \alpha_2, \alpha_3, \alpha_4)$ , and  $\mathcal{P} = (\mathcal{P}_1, \mathcal{P}_2, \mathcal{P}_3)$ . In contrast to TBM, the proposed THBM accounts for the ‘individual heterogeneity’ in terms of the variations in capture probabilities considering  $\mathcal{P}_s = \frac{\exp(b_s)}{1+\exp(b_s)}$  as a function of random effects  $b_s$  for  $s = 1, 2, 3$ . Now, integrating the likelihood function, given in (3), with respect to the distribution of random effects  $b_s$ , we obtain the marginal likelihood function of  $\boldsymbol{\theta}$  as

$$L(\boldsymbol{\theta}|\mathbf{x}) = \int_{\mathbb{R}^3} L(N, \boldsymbol{\alpha}, \mathcal{P}|\mathbf{x}) \times \left\{ \prod_{s=1}^3 g_{b_s}(b_s|\delta_s) \right\} db_1 db_2 db_3, \quad (4)$$

where  $\boldsymbol{\theta} = (N, \boldsymbol{\alpha}, \boldsymbol{\delta})$ , and  $g_{b_s}(\cdot|\delta_s)$  is a suitably chosen density function (e.g. Gaussian, logistic, etc.) of  $b_s$ ’s with the unknown real-valued parameter or parameter vector  $\delta_s$  for  $s = 1, 2, 3$ . In the conventional frequentist approach, computational challenges arise in the model fitting due to intractable numerical integration involved in the aforementioned log-likelihood function (Coul and Agresti, 1999). Using Gaussian quadrature or Laplace’s method, one can consider quasi-likelihood approaches or approximation methods for numerical integration. Alternatively, a Bayesian estimate of the parameters of interest can be obtained using the Metropolis-Hastings algorithm.

### 3.1 Identifiability Issues

The model parameters associated with THBM are not identifiable with respect to TRS data. In a frequentist setup, the performance of point estimation in the absence of identifiability may yield unsatisfactory results such as non-uniqueness of maximum likelihood estimates (White, 1982; Aldrich, 2002). To avoid the issues related to identifiability, Chatterjee and Bhuyan (2020a) considered two submodels TBM-1 and TBM-2 of TBM keeping  $\alpha_3$  and  $\alpha_4$  fixed as 0, respectively. Similar restrictions on parameters are also considered in the model  $M_{tb}$  and log-linear models as well as in the sample coverage approach proposed by Chao and Tsay (1998). However, this process of model contraction may lead to a model that involves dubious assumptions or a model that is less realistic in some other way (Gustafson, 2005). For example, available sources in epidemiological surveillance are not time ordered (Chao et al., 2001), and the capture attempts are supposed to be interdependent between themselves (Tsay and Chao, 2001; Ruche et al., 2013). Hence, the dependence between the first and third lists may be present, unlike the situation that is modelled by TBM-1. Similarly, TBM-2 is unsuitable

for scenarios when the second-order interaction among the lists is present. On the other hand, non-identifiability is not seen as a big obstacle to performing inferential procedures in the Bayesian paradigm (Wechsler et al., 2013). Infusing crude prior information into a non-identifiable model is considered an alternative to achieving identifiability through a model contraction. It is important to note that a non-identifiable model may bring information about the parameters of interest, and identifiable models do not necessarily lead to better decision-making than non-identifiable ones (Gustafson, 2005; Wechsler et al., 2013). In the following subsection, we propose a Bayesian estimation methodology of the parameter of interest  $N$  and associated parameters of the THBM under different choices of prior specifications on the nuisance parameters. Later, we also demonstrate that the proposed estimate of  $N$  is not sensitive to those prior specifications and outperforms existing competitors through an extensive simulation study (see Section 4).

### 3.2 Bayesian Approach

We propose a Bayesian estimation of the model parameters involved in the THBM given by (1) and (2), using the MCMC algorithm based on data augmentation. Unlike the usual frequentist setup, the proposed Bayesian approach provides a natural framework for prediction over unobserved data. Thus, by generating posterior predictive densities, rather than point estimates, we can make probability statements giving greater flexibility in presenting results. For instance, we can discuss findings concerning specific hypotheses or in terms of credible intervals which can offer a more intuitive understanding for the practitioners.

As mentioned before, the likelihood function  $L(\boldsymbol{\theta}|\mathbf{x})$ , given by (4), is not mathematically tractable due to the involvement of an integral and the additive structure of the cell probabilities  $p_{ijk}$  impose further challenges. One can apply the Metropolis-Hastings algorithm to generate samples from the posterior distribution of the model parameters  $\boldsymbol{\theta}$ , however, such computationally intensive methods are time inefficient and not appealing for the practitioners. To avoid such difficulty, we first attempt to simplify the likelihood function by taking a cue from the data augmentation strategy as suggested by Tanner and Wong (1987). Data augmentation refers to a scheme of augmenting the observed data so that it is easier to analyse. From a Bayesian point of view, this strategy may help to obtain an explicitly known form of conditional posterior distributions of the parameters of interest. For this purpose, we partition

the cell counts  $x_{ijk}$  depending on the various types of list dependence as described in (1), and define a vector of latent cell counts as:

$$\mathbf{y} = \left\{ y_{ijk,u} : \sum_{u=1}^{\nu} y_{ijk,u} = x_{ijk}; i, j, k = 0, 1; u = 1, \dots, \nu; \nu = 5^{\eta} 2^{1-\eta}; \eta = \mathcal{I}(i = j = k) \right\}.$$

where  $\mathcal{I}(\cdot)$  is an indicator function. For example,  $x_{111}$  can arise from all the five types of dependence structures, whereas  $x_{110}$  can be generated only based on the first and last types of dependence structures, as presented in (1). We also treat the random effects  $\mathbf{b} = (b_1, b_2, b_3)$  as unobserved data. Therefore, the likelihood function of  $\boldsymbol{\theta}$ , based on the complete data  $(\mathbf{x}, \mathbf{y}, \mathbf{b})$ , is given by

$$\mathcal{L}_c(\boldsymbol{\theta} | \mathbf{x}, \mathbf{y}, \mathbf{b}) = \mathcal{L}_c(N, \boldsymbol{\alpha}, \mathbf{b} | \mathbf{x}, \mathbf{y}) \times \left\{ \prod_{s=1}^3 g_{b_s}(b_s | \delta_s) \right\}, \quad (5)$$

where

$$\begin{aligned} \mathcal{L}_c(N, \boldsymbol{\alpha}, \mathbf{b} | \mathbf{x}, \mathbf{y}) \propto & \frac{N!}{(N-n)!} [(1-\alpha_0)\mathcal{P}_1\mathcal{P}_2\mathcal{P}_3]^{y_{111,1}} \times [\alpha_1\mathcal{P}_1\mathcal{P}_3]^{y_{111,2}} \times [\alpha_2\mathcal{P}_1\mathcal{P}_2]^{y_{111,3}} \times [\alpha_3\mathcal{P}_1\mathcal{P}_2]^{y_{111,4}} \\ & \times [\alpha_4\mathcal{P}_1]^{x_{111}-\sum_{i=1}^4 y_{111,i}} \times [(1-\alpha_0)\mathcal{P}_1\mathcal{P}_2(1-\mathcal{P}_3)]^{y_{110,1}} \times [\alpha_1\mathcal{P}_1(1-\mathcal{P}_3)]^{x_{110}-y_{110,1}} \\ & \times [(1-\alpha_0)(1-\mathcal{P}_1)\mathcal{P}_2\mathcal{P}_3]^{y_{011,1}} \times [\alpha_2(1-\mathcal{P}_1)\mathcal{P}_2]^{x_{011}-y_{011,1}} \\ & \times [(1-\alpha_0)\mathcal{P}_1(1-\mathcal{P}_2)(1-\mathcal{P}_3)]^{y_{100,1}} \times [\alpha_2\mathcal{P}_1(1-\mathcal{P}_2)]^{x_{100}-y_{100,1}} \\ & \times [(1-\alpha_0)\mathcal{P}_1(1-\mathcal{P}_2)\mathcal{P}_3]^{y_{101,1}} \times [\alpha_3\mathcal{P}_1(1-\mathcal{P}_2)]^{x_{101}-y_{101,1}} \\ & \times [(1-\alpha_0)(1-\mathcal{P}_1)\mathcal{P}_2(1-\mathcal{P}_3)]^{y_{010,1}} \times [\alpha_3(1-\mathcal{P}_1)\mathcal{P}_2]^{x_{010}-y_{010,1}} \\ & \times [(1-\alpha_0)(1-\mathcal{P}_1)(1-\mathcal{P}_2)\mathcal{P}_3]^{y_{001,1}} \times [\alpha_1(1-\mathcal{P}_1)\mathcal{P}_3]^{x_{001}-y_{001,1}} \\ & \times [(1-\alpha_0)(1-\mathcal{P}_1)(1-\mathcal{P}_2)(1-\mathcal{P}_3)]^{y_{000,1}} \times [\alpha_1(1-\mathcal{P}_1)(1-\mathcal{P}_3)]^{y_{000,2}} \\ & \times [\alpha_2(1-\mathcal{P}_1)(1-\mathcal{P}_2)]^{y_{000,3}} \times [\alpha_3(1-\mathcal{P}_1)(1-\mathcal{P}_2)]^{y_{000,4}} \times [\alpha_4(1-\mathcal{P}_1)]^{N-n-\sum_{i=1}^4 y_{000,i}}. \end{aligned}$$

Interestingly, the complete data likelihood, given by (5), possesses a simple form as a product of the power functions of the parameters associated with the THBM. Hence, the joint posterior density of all the unobserved quantity in the model  $\boldsymbol{\theta}$ ,  $\mathbf{y}$ , and  $\mathbf{b}$  given the observed data  $\mathbf{x}$  is provided by

$$\pi(\boldsymbol{\theta}, \mathbf{b}, \mathbf{y} | \mathbf{x}) \propto \mathcal{L}_c(\boldsymbol{\theta} | \mathbf{x}, \mathbf{y}, \mathbf{b}) \times \pi(\boldsymbol{\theta}), \quad (6)$$

where  $\pi(\boldsymbol{\theta})$  denotes the prior for  $\boldsymbol{\theta}$ . Following [Tanner and Wong \(1987\)](#), we employ a simple iterative algorithm to generate samples from the posterior density of  $\boldsymbol{\theta}$ . To implement the following steps, one must be able to sample from the conditional posterior distributions of  $\boldsymbol{\theta}$  given  $(\mathbf{x}, \mathbf{y}, \mathbf{b})$ ,  $\mathbf{y}$  given  $(\boldsymbol{\theta}, \mathbf{x}, \mathbf{b})$ , and  $\mathbf{b}$  given  $(\boldsymbol{\theta}, \mathbf{x}, \mathbf{y})$ , denoted by  $\pi(\boldsymbol{\theta}|\mathbf{x}, \mathbf{y}, \mathbf{b})$ ,  $\pi(\mathbf{y}|\boldsymbol{\theta}, \mathbf{x}, \mathbf{b})$ , and  $\pi(\mathbf{b}|\boldsymbol{\theta}, \mathbf{x}, \mathbf{y})$ , respectively.

Step 1. Set  $t = 0$  and initialize  $(\mathbf{y}^{(t)}, \mathbf{b}^{(t)})$ .

Step 2. Generate  $\boldsymbol{\theta}^{(t+1)}$  from  $\pi(\boldsymbol{\theta}|\mathbf{x}, \mathbf{y}^{(t)}, \mathbf{b}^{(t)})$ .

Step 3. Generate  $\mathbf{y}^{(t+1)}$  from  $\pi(\mathbf{y}|\boldsymbol{\theta}^{(t+1)}, \mathbf{x}, \mathbf{b}^{(t)})$ , and then  $\mathbf{b}^{(t+1)}$  from  $\pi(\mathbf{b}|\boldsymbol{\theta}^{(t+1)}, \mathbf{x}, \mathbf{y}^{(t+1)})$ .

Step 4. Update  $(\mathbf{y}^{(t)}, \mathbf{b}^{(t)})$  with  $(\mathbf{y}^{(t+1)}, \mathbf{b}^{(t+1)})$ .

Step 5. Repeat Step 2-4 until convergence of  $\left\{\boldsymbol{\theta}^{(t)}\right\}_{t \geq 0}$ .

Note that the conditional distribution  $\pi(\mathbf{y}|\boldsymbol{\theta}, \mathbf{x}, \mathbf{b})$  of the unobserved data  $\mathbf{y}$ , is expressed as a product of multinomial and binomial distributions. See Section 3.1 of the Supplementary Materials for details. Now, one can easily execute the above steps using Gibbs sampling if the full conditional distributions of  $\mathbf{b}$  and  $\boldsymbol{\theta}$  can be obtained in closed forms. In the next subsection, we propose appropriate priors for  $\boldsymbol{\theta}$  and suitable distribution of the random effects  $\mathbf{b}$ , so that the conditional posteriors  $\pi(\boldsymbol{\theta}|\mathbf{b}, \mathbf{y}, \mathbf{x})$  and  $\pi(\mathbf{b}|\boldsymbol{\theta}, \mathbf{y}, \mathbf{x})$  result in standard distributions.

### 3.2.1 Prior Specifications

We first assume the random effect  $b_s$  follows generalized logistic type-I distribution ([Johnson et al., 1994](#)) with shape parameter  $\delta_s$  for  $s = 1, 2, 3$ . This is among the few distributions which can model both positively and negatively skewed data on the whole real line. With this specific choice of distribution, the conditional posterior distribution of  $\mathbf{b}$  given  $(\boldsymbol{\theta}, \mathbf{x}, \mathbf{y})$  is obtained as

$$\pi(b_s|\boldsymbol{\theta}, \mathbf{x}, \mathbf{y}) \propto EGB2(n_s + 1, m_s + \delta_s), \quad s = 1, 2, 3,$$

where  $EGB2$  denotes for exponential generalized beta distribution of second kind ([Fischer, 2000](#)) with parameters involving  $m_1 = x_{1..}$ ,  $m_2 = y_{111,1} + y_{111,3} + y_{111,4} + y_{110,1} + x_{011} + x_{010}$ ,  $m_3 = y_{111,1} + y_{111,2} + y_{011,1} + y_{101,1} + x_{001}$ ,  $n_1 = N - x_{1..}$ ,  $n_2 = x_{100} + x_{101} + y_{001,1} + y_{000,1} + y_{000,3} + y_{000,4}$ , and  $n_3 = x_{110} + y_{100,1} + y_{010,1} + y_{000,1} + y_{000,2}$ . See Section 3.2 of the Supplementary

Materials for detailed derivation. Now, one can easily sample from  $\pi(b_s|\boldsymbol{\theta}, \mathbf{x}, \mathbf{y})$  and compute  $\mathcal{P}_s = [1 + \exp(-b_s)]^{-1}$  for  $s = 1, 2, 3$ .

For our analysis, the prior on  $\boldsymbol{\theta} = (N, \boldsymbol{\alpha}, \boldsymbol{\delta})$  are assigned in (6) independently, i.e.  $\pi(\boldsymbol{\theta}) = \pi(N)\pi(\boldsymbol{\alpha})\pi(\boldsymbol{\delta})$ . We propose both informative and noninformative priors for the nuisance parameters  $\boldsymbol{\alpha}$  and  $\boldsymbol{\delta}$  with noninformative prior on the parameters of interest  $N$ . These different prior choices enable us to study the robustness of the proposed inferential methodology and provide flexibility to the users. The two different choices of the priors and associated conditional posterior distribution of  $\boldsymbol{\theta}$  are provided below.

### Prior Choice I

As discussed before, we first consider noninformative priors for the purpose of Bayesian estimation. The Jeffrey's priors for all the parameters involved in THBM are given by  $\pi(N) \propto N^{-1}$ ,  $\pi(\boldsymbol{\alpha}) \equiv \pi(\alpha_1, \alpha_2, \alpha_3, \alpha_4, \alpha_5) \propto \text{Dirichlet}(0.5, 0.5, 0.5, 0.5, 0.5)$ , where  $\alpha_5 = 1 - \alpha_0$  and  $\pi(\delta_s) \propto \delta_s^{-1}$  for  $s = 1, 2, 3$ . Under these choices, the full conditional densities of  $\boldsymbol{\alpha}$  and  $\delta_s$ 's are obtained as

$$\begin{aligned}\pi(\boldsymbol{\alpha}|\boldsymbol{\theta}_{-\boldsymbol{\alpha}}, \mathbf{x}, \mathbf{y}, \mathbf{b}) &\propto \text{Dirichlet}(\mathbf{d}), \\ \pi(\delta_s|\boldsymbol{\theta}_{-\delta_s}, \mathbf{x}, \mathbf{y}, \mathbf{b}) &\propto \text{Exponential}(w_s), \quad s = 1, 2, 3,\end{aligned}$$

where  $\mathbf{d} = (d_1, d_2, d_3, d_4, d_5)$  with  $d_1 = y_{111,2} + x_{110} - y_{110,1} + x_{001} - y_{001,1} + y_{000,2} + 0.5$ ,  $d_2 = y_{111,3} + x_{011} - y_{011,1} + x_{100} - y_{100,1} + y_{000,3} + 0.5$ ,  $d_3 = y_{111,4} + x_{101} - y_{101,1} + x_{010} - y_{010,1} + y_{000,4} + 0.5$ ,  $d_4 = x_{111} - \sum_{u=1}^4 y_{111,u} + N - n - \sum_{u=1}^4 y_{000,u} + 0.5$ ,  $d_5 = y_{111,1} + y_{110,1} + y_{011,1} + y_{100,1} + y_{101,1} + y_{010,1} + y_{001,1} + y_{000,1} + 0.5$ , and  $w_s = \log[1 + \exp(-b_s)]$ . The full conditional distribution of the parameter of interest  $N$  is given by

$$\begin{aligned}\pi(N|\boldsymbol{\theta}_{-N}, \mathbf{x}, \mathbf{y}_{-y_{000,5}}, \mathbf{b}) &\propto \frac{(N-1)!}{(N-n-\sum_{u=1}^4 y_{000,u})!} [\alpha_4(1-\mathcal{P}_1)]^{N-n-\sum_{u=1}^4 y_{000,u}}, \\ \text{i.e. } \pi(y_{000,5}|\boldsymbol{\theta}_{-N}, \mathbf{x}, \mathbf{y}_{-y_{000,5}}, \mathbf{b}) &\propto NB\left(n + \sum_{u=1}^4 y_{000,u}, 1 - \alpha_4(1-\mathcal{P}_1)\right),\end{aligned}\tag{7}$$

where  $y_{000,5} = N - n - \sum_{u=1}^4 y_{000,u}$ , and NB denotes for negative binomial distribution. The detailed derivations of the full conditional distributions are provided in Sections 3.3-3.5 of the Supplementary Material. Now, one can easily execute the algorithm provided in Section 3.2 to generate a sample from the posterior distribution  $\boldsymbol{\theta}$  using Gibbs sampling. Therefore,

summary statistics of the posterior distribution can be used to find a point estimate of  $N$  based on a suitable choice of loss function. We refer to this estimate as THBM-I. The associated R-programme is provided in Section 5 of the Supplementary Material.

## Prior Choice II

Here, we consider informative priors on  $\boldsymbol{\alpha}$  and  $\boldsymbol{\delta}$ , and Jeffrey's prior for the parameter of interest  $N$  is considered as before. Based on the subjective choices of the hyperparameters, we propose Dirichlet prior for  $\boldsymbol{\alpha}$  with parameter vector  $(\beta_1, \beta_2, \beta_3, \beta_4, \beta_5)$ , and gamma prior for  $\delta_s$  with scale  $\lambda_s$  and shape  $\gamma_s$ , for  $s = 1, 2, 3$ . Here also, the full conditional distributions of  $\boldsymbol{\alpha}$  and  $\delta_s$  posses closed form expressions and are given by

$$\begin{aligned}\pi(\boldsymbol{\alpha}|\boldsymbol{\theta}_{-\boldsymbol{\alpha}}, \mathbf{x}, \mathbf{y}, \mathbf{b}) &\propto \text{Dirichlet}(\mathbf{d}^*), \\ \pi(\delta_s|\boldsymbol{\theta}_{-\delta_s}, \mathbf{x}, \mathbf{y}, \mathbf{b}) &\propto \text{Gamma}\left(\gamma_s + 1, \left(w_s + \frac{1}{\lambda_s}\right)^{-1}\right), \quad s = 1, 2, 3,\end{aligned}$$

where  $\mathbf{d}^* = (d_1^*, d_2^*, d_3^*, d_4^*, d_5^*)$  with  $d_u^* = d_u - 0.5 + \beta_u$  for  $u = 1, 2, \dots, 5$ . The derivations of the full conditional distributions are provided in Sections 3.3-3.5 of the Supplementary Material. In order to consider diffuse prior on  $\delta_s$ , one can choose the hyperparameters  $\gamma_s$  and  $\lambda_s$  appropriately such that the variance of the prior distribution is large. The conditional posterior distribution of  $N$  remains the same as provided in (7). Here also, the full conditionals are from a standard family of distributions and one can use a Gibbs sampler for inferential purposes and the resulting estimates are referred to as THBM-II.

## 4 Simulation Study

In this section, we evaluate the performances of the proposed estimators under the two prior setups in the presence of list dependence due to behavioural change and individual heterogeneity through an extensive simulation study. We compare the results to the following relevant competitors that account for the list dependence or/and individual heterogeneity: (I) List dependence only–log-linear model (LLM) with interaction effects (Fienberg, 1972) and model  $M_{tb}$  (Chao et al., 2000; Chatterjee and Bhuyan, 2020a); (II) Heterogeneity only–quasi-symmetry model (QSM) (Darroch et al., 1993), partial quasi-symmetry model (PQSM) (Darroch et al.,

1993) and Bayesian non-parametric latent class model (NPLCM) (Manrique-Vallier, 2016b); (III) Both list dependence and heterogeneity–  $M_{bh}$  model (Rivest and Levesque, 2001) and non-parametric sample coverage method (SC) (Chao and Tsay, 1998); and (IV) List independence and homogeneity: the log-linear model without interaction effects (IM) (Fienberg, 1972). The details of all these existing models and associated estimates are briefly presented in Section 2 of the Supplementary Material.

We consider six different choices of  $(\alpha_1, \alpha_2, \alpha_3, \alpha_4, \alpha_5)$  representing varying degrees of list dependence and denote them as P1-P6 the in Table 1. We generate TRS data from the proposed model keeping the total population size  $N$  fixed at 200 and 500 for each of these six different choices of populations P1-P6 with five different combinations of random effects characterized by  $\delta$  given as  $(1.6, 1.2, 0.8)$ ,  $(1.3, 1.7, 0.9)$ ,  $(1.0, 1.4, 1.8)$ ,  $(0.8, 0.8, 0.8)$ ,  $(1.6, 1.6, 1.6)$ . The choices of  $N$  are similar to the population sizes of the case studies under consideration. Note that  $\delta = (0.8, 0.8, 0.8)$  and  $(1.6, 1.6, 1.6)$  present the cases where capture probabilities of the causally independent individuals in all the three lists are identically distributed. In contrast, the capture probabilities differ from one list to another for the other three choices of  $\delta$ .

Table 1: Dependence structure of the simulated populations.

Population	$(\alpha_1, \alpha_2, \alpha_3, \alpha_4, \alpha_5)$
P1	$(0.35, 0.15, 0.25, 0.10, 0.15)$
P2	$(0.30, 0.30, 0.15, 0.10, 0.15)$
P3	$0.20, 0.10, 0.20, 0.10, 0.40)$
P4	$(0.10, 0.20, 0.30, 0.20, 0.20)$
P5	$(0.20, 0.20, 0.20, 0.20, 0.20)$
P6	$(0.25, 0.15, 0.35, 0.10, 0.15)$

Note that  $\alpha_5 = 1 - \alpha_0$ .

We consider two different sets of prior as discussed in the Subsection 3.2.1 for estimation of the proposed model. Jeffrey’s priors (Prior Choice I) are considered in THBM-I, and for THBM-II, we consider  $\beta_u = 8\alpha_u$  for  $u = 1, 2, \dots, 5$ , and diffuse prior for  $\delta_s$  using gamma distribution with mean  $\delta_s$  and variance 100, for  $s = 1, 2, 3$  (Prior Choice II). We generate a chain with 50,000 samples from the posterior distributions of the parameters associated with THBM using Gibbs sampling and find the posterior median of the population size based on

every 10th iterate discarding the first 25,000 iterations as burn-in. The thinning interval of size 10 reduces the dependency among the samples at a satisfactory level, and the convergence of the chains is monitored using Geweke's diagnostic test (Geweke, 1992). This is repeated 1000 times and the average estimates  $\hat{N}$  are reported in Tables S3-S8 provided in Section 4 of the Supplementary Material. We also report the 95% highest posterior density (HPD) credible interval along with coverage probability (CP) of  $N$  and the Relative Mean Absolute Error, defined as  $RMAE = \frac{1}{1000} \sum_{r=1}^{1000} \left| \frac{\hat{N}_r - N}{N} \right|$ , where  $\hat{N}_r$  denotes the estimate based on data generated at the  $r$ th replication. Similarly, we compute the RMAE of all the existing competitors. For each of these 1000 replications, 95% confidence intervals (CI) of  $N$  for these competitive methods are obtained based on the quantiles from 1000 bootstrap samples. The CP of the population size  $N$  is also obtained based on the bootstrap CIs.

The proposed model performs the best in terms of RAME for all the simulated populations P1-P6 for both  $N = 200$  and  $N = 500$ . Moreover, the CPs of the proposed estimates are higher than all the existing competitors except  $M_{tb}$  model which possesses a very wide CI due to high variability. In most of the cases, the CP of QSM and PQSM estimates are comparable for  $N = 200$  but CP of PQSM estimate is lower than QSM estimate for  $N = 500$ . The CP of LLM estimate is lower than PQSM estimates for both  $N = 200$  and  $N = 500$ . It is important to note that the CIs associated with the independent model and the SC estimates are very tight and which results in extremely low CPs. In contrast, the CI-width based on  $M_{bh}$  are exorbitantly large in most cases and with negative lower limits on many occasions. In particular, the CPs of the SC estimates are less than 6% for P4 and P5 (see Tables S6-S7 in Section 4 of the Supplementary Material), and the highest is around 55% attained for only two cases in P3 with  $N = 200$  (see Table S5 in Section 4 of the Supplementary Material). Similar results for NPLCM and  $M_{bh}$  are also observed in a few cases. Also, the IM, SC, and NPLCM consistently underestimate  $N$  for all populations P1-P6. Interestingly, the  $M_{tb}$  model underestimates for P4 and P5 and overestimates for the rest of the populations. It is also observed that the RAME of all the estimators except the independent model and SC method decreases as  $N$  increases from 200 to 500 for all simulated populations P1-P6.

As discussed in Section 2.3.1 of the Supplementary Material, we have observed that the SC estimate suffers from boundary problems in our simulation study. It is easy to generate data such that the percentage of infeasible estimates is as high as 60% to 80%. In some other cases, we have also observed that the QSM, PQSM, and LLM may fail to converge and produce

extremely large estimates. For a valid and fair comparison, we have not reported those cases here.

## 4.1 Sensitivity Analysis

### 4.1.1 Sensitivity of Prior Specification

As discussed before, the proposed estimates of the population size  $N$  based on two different sets of priors perform better than the existing competitors. But to understand the sensitivity of the estimate with prior specifications, we now compare the results associated with THBM-I and THBM-II in Tables S3-S8 (see Section 4 of the Supplementary Material). In general, the CPs of the estimates of  $N$  with both the prior specifications are very similar, but only in a few cases, CPs of THBM-I are marginally lower than those of THBM-II. Although the performance of the THBM-II is better than THBM-I for all the simulated populations P1-P6 in terms of RMAE, the difference is merely less than 3%. The marginal improvement is due to the fact that the prior variance of  $\alpha_i$ 's considered in THBM-II is considerably smaller compared to the variance of Jeffrey's prior in THBM-I. From these observations, it indicates that the proposed methodology is not sensitive to prior specifications, and these are especially valuable when only limited prior information is available.

### 4.1.2 Sensitivity of Random Effects

In the posed estimation methodology, we are obliged to assume that the random effects  $b_s$ 's follow generalized logistic distribution to obtain a closed-form expression of the full conditionals. However, this assumption may not be valid in real applications and it is worth investigating the effect of misspecification of random effects distributions on the performance of the proposed estimate. For this purpose, we generate data for populations P1-P6 considering random effects from generalized logistic type-I ( $GL_I$ ), normal and, gamma distributions with two different parameter choices provided in Table 2. The RAMEs and CPs of THBM-I are plotted in Figure 1 and Figure 2, respectively. Similar patterns are observed for THBM-II (not reported here). In terms of RAME, we observe minor deterioration due to misspecification when the true random effects are generated from gamma distributions, but in contrast, marginal improvement is observed when random effects are generated from the normal distributions. In all the

six populations P1-P6, the range of differences in RAMEs is only less than 3% (see Figure 1). However, no effect of misspecification is noticed on CPs in any of the six populations (see Figure 2). We also consider random effects for discrete distribution, and the results are similar to the aforementioned cases (not reported here).

Table 2: Random effects distributions for analysing sensitivity of misspecification.

Random Effects	$b_1$	$b_2$	$b_3$
R1	$GL_I(1.6)$	$GL_I(1.6)$	$GL_I(1.6)$
R2	$GL_I(1.6)$	$GL_I(1.2)$	$GL_I(0.8)$
R3	$Normal(0.5, 1)$	$Normal(0.5, 1)$	$Normal(0.5, 1)$
R4	$Normal(0.5, 1)$	$Normal(0, 1)$	$Normal(-0.5, 1)$
R5	$Gamma(2, 0.5)$	$Gamma(2, 0.5)$	$Gamma(2, 0.5)$
R6	$Gamma(2, 0.5)$	$Gamma(1, 0.5)$	$Gamma(0.5, 0.5)$

$GL_I(\eta)$  denotes generalized logistic type-I distribution with parameter  $\eta$ .

$Normal(\mu, \sigma)$  denotes normal distribution with mean  $\mu$  and standard deviation  $\sigma$ .

$Gamma(a, b)$  denotes gamma distribution with shape parameter  $a$  and scale parameter  $b$ .

#### 4.1.3 Sensitivity of Model Misspecification

As discussed in Section 2, the proposed model represents a realistic mechanism to account for inherent heterogeneity among the individuals and dependencies. Nevertheless, it is important to study the effect of model misspecification when the data-generating mechanism deviates from the assumed structure of the fitted model. For this purpose, we generate the capture statuses of the individuals  $Z_h^{(1)}, Z_h^{(2)}, Z_h^{(3)}$  from Bernoulli distributions with respective probabilities  $P_h^{(1)}, P_h^{(2)}$ , and  $P_h^{(3)}$ , where  $P_h^{(j)} = \min\{P_h^{(j-1)}\mathbb{I}[Z_h^{(j-1)} = 0] + 1.2\mathbb{I}[Z_h^{(j-1)} = 1], 0.99\}$ , for  $j = 2, 3$ , and  $h = 1, \dots, N$ . This mechanism induces a dependence structure among the capture statuses similar to a first-order auto-regressive model. To incorporate heterogeneity in the capture probabilities, we generate  $P_h^{(1)}$ 's from three different choices of distributions: (i)  $Uniform(0, 1)$ , (ii)  $Beta(4, 2)$ , and (iii)  $Beta(2, 2)$ . The RAMEs and CPs of THBM-I and its competitors are plotted in Figure 3 and Figure 4, respectively. In most of cases, the proposed estimator outperforms the existing competitors with respect to RAME. The CPs of the proposed estimator and  $M_{tb}$  model are close to 100% and much better than all other estimators.

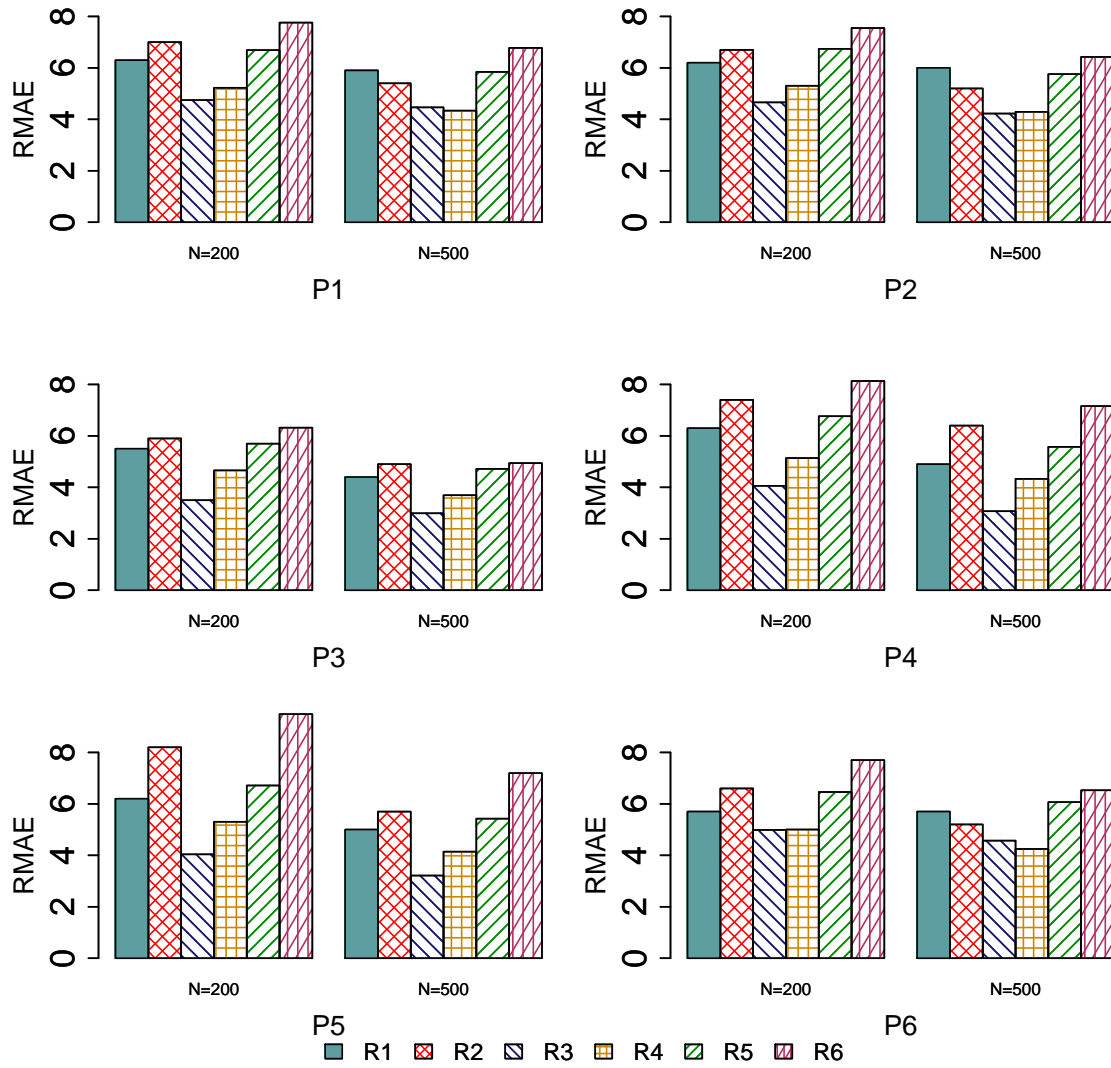


Figure 1: Comparison of RAMEs (in %) of the proposed estimate under different random effects models for data generation.

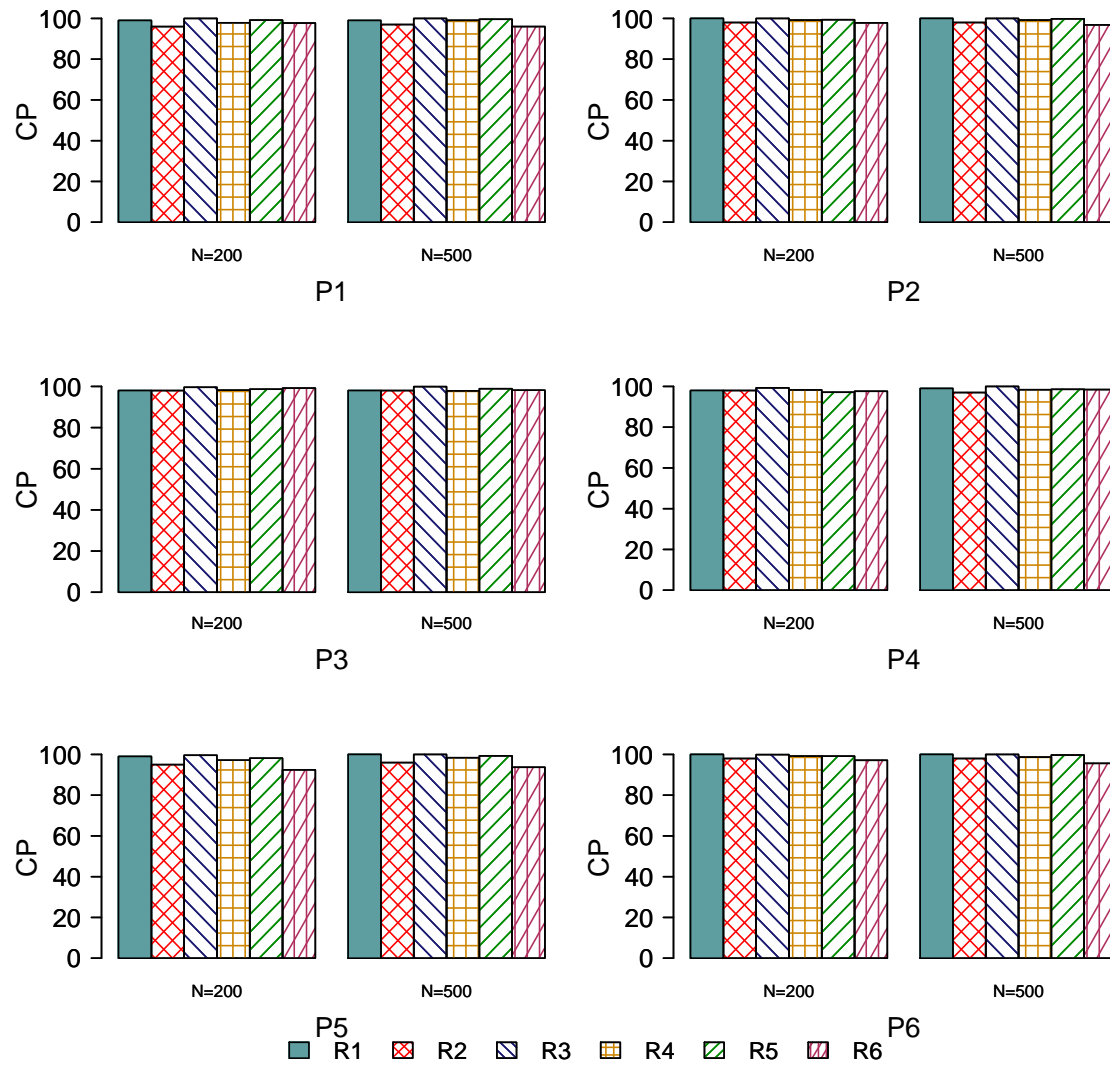


Figure 2: Comparison of CPs (in %) of the proposed estimate under different random effects models for data generation.

In particular, the performance of SC is very poor and its CPs are less than 40% in all the cases.

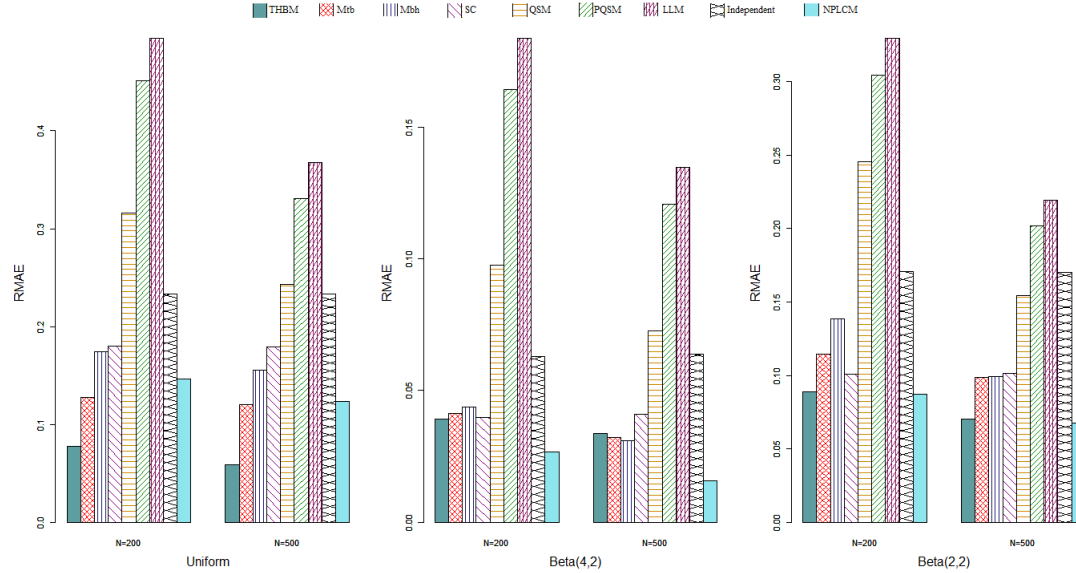


Figure 3: Comparison of the RAMEs (in %) of the proposed estimate with the existing competitors under model misspecification when data generated from auto-regressive dependence structure with capture probabilities  $P_h^{(1)}$ 's in the list  $L_1$  follow (i)  $Uniform(0, 1)$ , (ii)  $Beta(4, 2)$ , and (ii)  $Beta(2, 2)$ .

## 5 Case Study

As discussed before, applications of MSE are commonly found in the domain of epidemiology. In this section, we consider two different case studies on infectious diseases. The results from analyses of the two datasets based on the proposed methodology are discussed below along with the practical implications. We also compare these results with the estimates based on the existing methods.

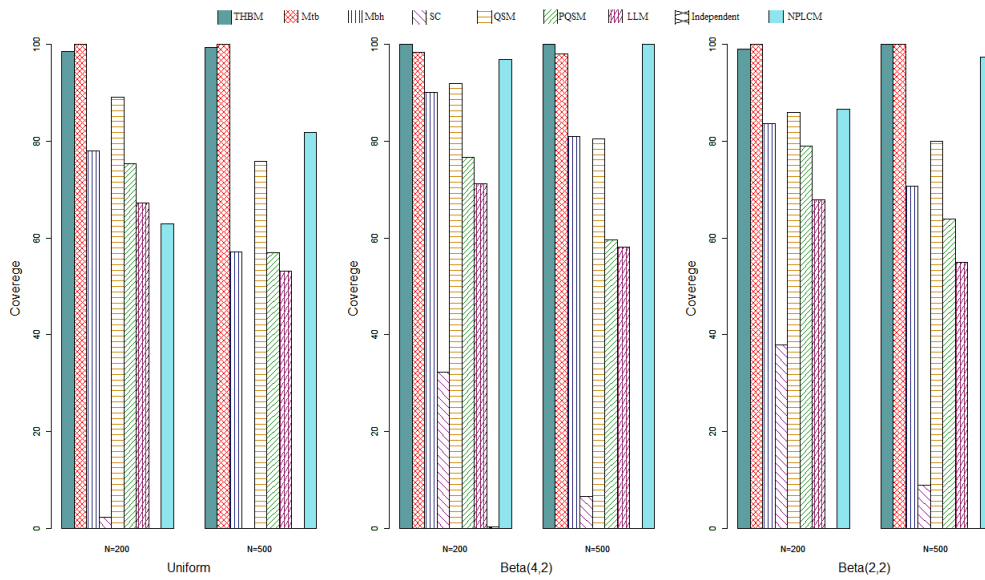


Figure 4: Comparison of the CPs (in %) of the proposed estimate with the existing competitors under model misspecification when data generated from auto-regressive dependence structure with capture probabilities  $P_h^{(1)}$ 's in the list  $L_1$  follow (i)  $Uniform(0, 1)$ , (ii)  $Beta(4, 2)$ , and (ii)  $Beta(2, 2)$ .

## 5.1 Analysis of Legionnaires' Disease Surveillance Data

As discussed in Section 1, we consider a dataset on the LD outbreak in the Netherlands in the year 1999. To apply the proposed methodology to estimate the total number of infected individuals, we consider Jeffrey's prior for all the parameters associated with THBM-I. For THBM-II, we consider Dirichlet prior for  $\alpha$  with parameter  $(0.2, 0.1, 0.1, 0.1, 0.5)$  and gamma prior for  $\delta_1, \delta_2, \delta_3$  with mean  $0.5, 0.5, 3$ , respectively, and variance  $100$ . We generate a chain with 1 million samples from the posterior distributions of the associated model parameters using the Gibbs sampling algorithm and discard the first 10% iterations as burn-in. The convergence of the chain is monitored graphically and using Geweke's diagnostic test (Geweke, 1992).

To reduce the extent of heterogeneity as well as the dependence that is induced by heterogeneity in the population, it is often recommended to employ post-stratification of the population based on appropriate demographic (e.g. age, race or sex) or geographic variables (Wolter, 1986; Islam, 2015). In this application, we estimate the prevalence of LD in four regions: North (1,671,534 inhabitants), East (4,467,527 inhabitants), West (5,955,299 inhabitants), and South (3,892,715 inhabitants) to facilitate regional surveillance and identification of associated risk factors. The results based on the proposed method are presented in Table 3. It is quite common to observe that the sum of the strata-wise estimate of the population sizes does not tally with the estimate obtained from the aggregated data if the underlining heterogeneity is not successfully accounted for. In this context of capture-recapture experiments, this phenomenon is popularly known as Simpson's paradox or simply Yule's association paradox (Kadane et al., 1999). The median, and the 95% HPD credible interval of  $N$  based on the aggregated data are also reported in Table 3. Interestingly, the estimate of the total LD incidence obtained by summing the four regional estimates approximately matches with the national estimate based on combined data. It is an indication that the proposed method successfully accounted for the heterogeneity present in the population. The estimate of  $N$  based on THBM-I is marginally larger than that of THBM-II. Interestingly, the length of the HPD credible interval is marginally shorter for THBM-II due to the use of informative prior for  $\alpha$  compared to that of the THBM-I, which in contrast, involves Jeffrey's prior. This observation is as expected based on the findings from our simulation study discussed in Subsection 4.1.1. We also observe that the estimates of  $N$  are similar under both Jeffrey's prior and informative

prior for  $\delta_l$ 's while considering Jeffrey's prior for  $\alpha$  (not reported here). We also report the estimates of  $N$  based on different existing methods. The CI's are computed based on 10,000 bootstrap samples. The estimates based on the IM, NPLCM, and SC method are considerably lower than other estimates. For all the regions,  $M_{bh}$  provides infeasible estimates (smaller than the total observed cell count  $n$ ), and  $M_{tb}$  and QSM provide very large estimates compared to other competitors.

To gain insight from our analysis, we present the posterior density of  $N$  and boxplot of the capture probabilities associated with DNR, Laboratory, and Hospital records in Figure 5(a), and Figure 5(b), respectively, based on aggregated data using THBM-I. The posterior density of  $N$  is slightly skewed toward the right and the catchability of Hospital records is considerably higher than those of DNR and Laboratory records. It is also seen that the heterogeneity in capture probability associated with Hospital records is higher compared to other sources. From Figures 5(c)-5(f), it is visible that the bulk of the distribution of all the dependence parameters is away from 0 which indicates their significance. The estimates of the dependence parameters suggest that almost 60% individuals are causally dependent, and 13% of individuals have perfect positive association among the three lists.

In Table 4, we also report the under-reporting rate (UR) and prevalence rate (PR)<sup>2</sup> for each of these four regions based on our estimate of the prevalence obtained from THBM-I. The estimated UR in the North and West are similar but marginally lower than that in the South. However, the estimated UR in the East is significantly higher than in other regions. We also observe that the CI associated with the estimate of LD incidence in the East is wide. This encourages further investigation, possibly involving information from other sources, to obtain a more reliable estimate. As mentioned before, the capture probability associated with Laboratory records is very low (see Figure 5(b)), and it is worth considering alternative sources with higher capture probability to improve the coverage. The PR is the highest in the South and least in the North. However, a marginal difference in PR is observed between East and West. Some previous studies suggest that weather and climatic conditions are associated with LD incidence (Karagiannis et al., 2009; Brandsema et al., 2014). On average, the northern provinces endure lower temperatures compared to the southern provinces. In particular, the east of Brabant and the very north of Limburg are the warmest during summer. Our analyses

---

<sup>2</sup>UR =  $\frac{(\hat{N} - n)}{\hat{N}} \times 100$ , PR =  $\frac{\hat{N}}{\text{No. of inhabitants}} \times 100,000$

indicate that warm weather increases LD incidence, which supports the findings by [Karagiannis et al. \(2009\)](#) and [Brandsema et al. \(2014\)](#). Recently, researchers are also interested in the association between LD incidence and precipitation and humidity ([Passer et al., 2020](#)). In general, there is no dry season in the Netherlands, and precipitation is common throughout the year. This is perhaps one of the major risk factors causing a higher PR in the Netherlands compared to other countries. In particular, the coastal provinces (West) experience the heaviest rain showers after the summer and during the autumn resulting in higher PR compared to the North. Several other factors related to demographics and socioeconomic characteristics may lead to a higher incidence of LD ([Farnham et al., 2014](#); [Passer et al., 2020](#)). Following a similar post-stratification strategy, as considered in this article, one can effectively support the general goals of surveillance. It helps to rapidly recognize cases that occur in similar locations and describe incidences and trends. Also, one can identify opportunities for prevention and monitor the effectiveness of interventions implemented as part of an outbreak investigation ([Centers for Disease Control and Prevention, 2021](#)).

Table 3: Summary results of the Legionnaires' disease surveillance data analysis.

Region	THBM-I	THBM-II	NPLCM	SC	QSM	PQSM	LLM	$M_{tb}$	$M_{bh}$	IM
North	$\hat{N}$ 95	82	79	85	173	98	97	213	20	74
	CI* ( 70, 168 )	( 69 , 137 )	( 69, 105 )	( 67, 122 )	( 81, 873 )	( 65, 12×10 <sup>10</sup> )	( 58, 228 )	( 80, 475 )	( 2, 23 )	( 65, 76 )
East	$\hat{N}$ 318	313	242	243	391	447	720	416	93	198
	CI* ( 216, 685 )	( 214, 537 )	( 189, 368 )	( 210, 292 )	( 253, 796 )	( 1.7×10 <sup>10</sup> , 70.3×10 <sup>10</sup> )	( 1043×10 <sup>10</sup> , 3504×10 <sup>10</sup> )	( 201, 790 )	( 27, 58 )	( 188, 214 )
West	$\hat{N}$ 387	363	346	363	672	433	419	714	78	315
	CI* ( 317, 492 )	( 307, 455 )	( 292, 436 )	( 319, 426 )	( 437, 1267 )	( 334, 919 )	( 303, 1236 )	( 334, 1284 )	( 17, 34 )	( 307, 346 )
South	$\hat{N}$ 308	283	274	287	540	304	308	674	103	257
	CI* ( 259, 401 )	( 254, 334 )	( 235, 346 )	( 257, 327 )	( 352, 1021 )	( 243, 441 )	( 256, 671 )	( 305, 1274 )	( 31, 56 )	( 237, 261 )
Total	$\hat{N}$ 1114	1106	980	992	1803	1176	1253	1400	351	855
	CI* ( 948, 1347 )	( 942, 1290 )	( 812, 1265 )	( 922, 1078 )	( 1387, 2509 )	( 923, 1363 )	( 986, 1614 )	( 1153, 2104 )	( 136, 178 )	( 829, 878 )

THBM: Trivariate Heterogeneous Bernoulli Model; SC: Sample Coverage; QSM: Quasi-symmetry Model; PQSM: Partial Quasi-symmetry Model; LLM: Log-linear Model,  $M_{tb}$ : Time Behavioural Response Variation Model;  $M_{bh}$ : Individual Heterogeneity and Behavioural Response Variation Model; IM: LLM without interaction effects.

\* For THBM-I, THBM-II, and NPLCM, CI refers to HPD Credible Interval.

## 5.2 Analysis of Hepatitis A Virus Surveillance Data

Here, we consider the surveillance data of the HAV outbreak in northern Taiwan in the year 1995 to estimate the total number of infected individuals. As before, we consider Jeffrey's prior for THBM-I. For THBM-II, we consider Dirichlet prior for  $\alpha$  with parameter  $(0.1, 0.1, 0.1, 0.2, 0.5)$  and gamma prior for  $\delta_s$  with mean 0.5 and variance 100 for  $s = 1, 2, 3$ .

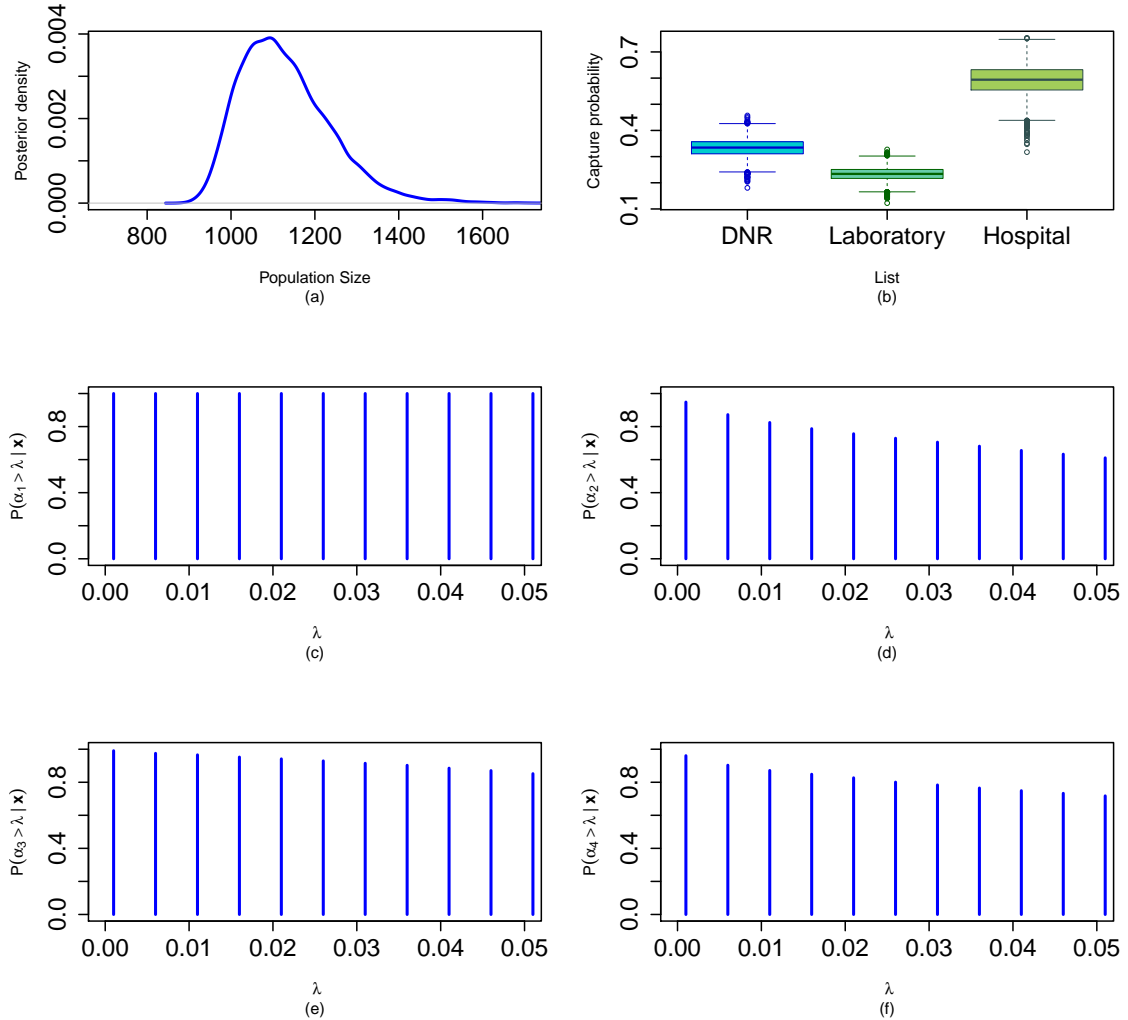


Figure 5: (a) Posterior density of the size of population affected with Legionnaires' disease; (b) Boxplots of capture probabilities associated with three different lists; (c) Test of significance of  $\alpha_1$ ; (d) Test of significance of  $\alpha_2$ ; (e) Test of significance of  $\alpha_3$ ; (f) Test of significance of  $\alpha_4$ .

Table 4: Region-wise prevalence rate and underreporting rate of the Legionnaires' disease based on THBM-I.

	North	South	East	West
PR	5.7	7.9	7.1	6.5
UR	27	32	42	26

PR: Prevalence rate per 100000 inhabitants; UR: Underreporting rate in %

For this purpose, we generate 5 million samples using the Gibbs sampling from the posterior distributions of the associated model parameters and discard the first 20% iterations as burn-in. Here also, no convergence issues are found based on Geweke's diagnostic test. The estimates of  $N$  along with 95% HPD credible interval based on both THBM-I and THBM-II are reported in Table 5. Here, the length of the HPD credible interval for  $N$  based on THBM-II is considerably smaller than that of THBM-I, in line with our findings in Subsections 4.1.1 and 5.1. We also provide the results based on the existing methods for comparison. Here also, the estimate based on the IM is considerably lower than other estimates. The proposed estimate is marginally larger than that of NPLCM and  $M_{tb}$  but lower than that of  $M_{bh}$ . The results based on QSM, PQSM, and LLM are much higher than the estimates based on THBM, NPLCM and  $M_{tb}$ . The estimates based on QSM, PQSM, and LLM are comparable but the CI of both QSM and PQSM is wider than that of LLM. Similar to our findings from simulation study, the CI width of  $M_{bh}$  is exorbitantly high. The estimated sample coverage  $\hat{C} = 51\%$  indicates the estimates provided by the SC method are not reliable.

Findings based on THBM-I are graphically presented in Figure 6. One can observe that the posterior distribution of  $N$  is highly skewed (see 6(a)). The catchability of all three lists is similar but the heterogeneity in capture probability associated with P-list (i.e. records based on a serum test) is marginally higher than that of the other lists (see Figure 6(b)). Cases of HAV are not clinically distinguishable from other types of acute viral hepatitis, which results in low capture probability in all the sources (World Health Organization, 2021). Here also, the bulk of the distribution of all the dependence parameters is significantly away from 0 (see Figure 6(c)-6(f)). Almost 29% individuals are causally dependent, and 15% of individuals have perfect positive associations among the three lists.

In December 1995, the National Quarantine Service of Taiwan conducted a screen serum

test for the HAV antibody for all students at the college at which the outbreak of the HAV occurred to determine the number of infected students. Based on their final figure, the estimated UR is 50% (Chao et al., 1997), but our estimate of the UR is 57%. Nevertheless, the level of underreporting of HAV cases is considerably high. As effective interventions to control the further spread of HAV are available, underreporting leads to serious consequences because it prevents prompt and effective public health action to protect immediate contacts of cases and their communities (Crowcroft et al., 2001). After this outbreak, Taiwan started to immunize children in 30 indigenous townships against HAV and further expanded to 19 non-indigenous townships with higher incidence or increased risk of epidemic in 1997-2002. It has been reported that the annual PR of HAV decreased from 2.96 in 1995 to 0.90 in 2003-2008. The PR in vaccinated townships and unvaccinated townships declined 98.3% and 52.6%, respectively (Tsou et al., 2011). This apparently indicates the long-term efficacy of the HAV vaccine in disease control in the vaccinated population and the out-of-cohort effect in the unvaccinated population. However, these figures do not account for the underreported cases, and any conclusion drawn from these statistics may be misleading. In particular, vaccination efficacy is overestimated when UR is higher in the vaccinated population compared to the unvaccinated population. Therefore, it is essential to estimate the underreported cases and adjust the calculation of PR (as considered in Subsection 5.1) for an unbiased evaluation of the interventions. For this purpose, the proposed model is a good choice to obtain an efficient estimate of the total number of individuals (or equivalently the underreported cases) infected by a disease such as HAV.

In 2003-2008, PR doubled in unvaccinated townships among those aged more than 30 years (Tsou et al., 2011). The lack of demographic or geographical information for this case study hampered our ability to carry out a stratified analysis. At the national level, geographical analysis of outbreaks can support surveillance and identification of associated risk factors. Without detailed risk factor information, it is difficult to develop and implement appropriate policies to contain the spread of this infection (Matin et al., 2006).

## 6 Discussions

This paper addresses the issue of population size estimation incorporating the possible list dependence arising from behavioural response variation and heterogeneous catchability. For

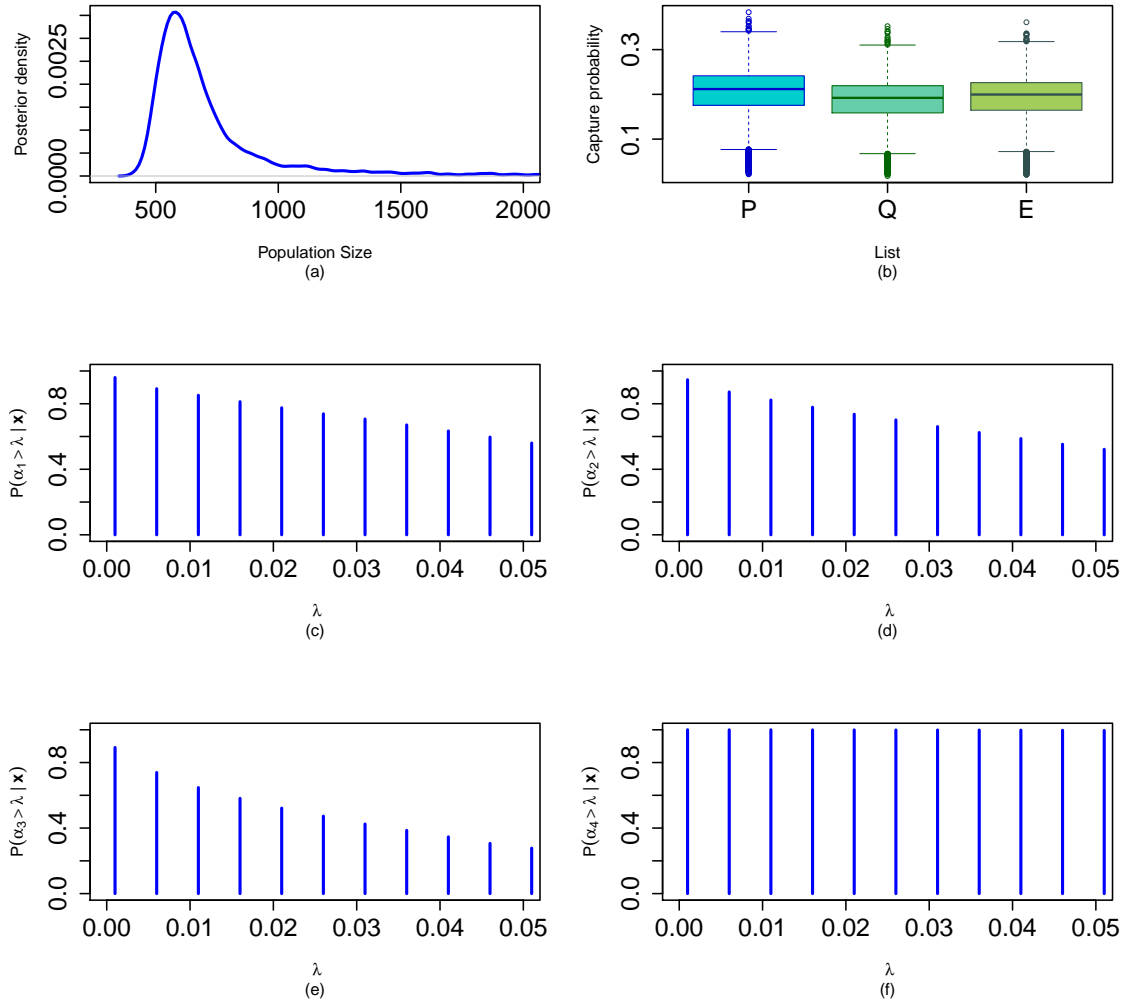


Figure 6: (a) Posterior density of the size of HAV infected population; (b) Box plots of capture probabilities associated with three different lists; (c) Test of significance of  $\alpha_1$ ; (d) Test of significance of  $\alpha_2$ ; (e) Test of significance of  $\alpha_3$ ; (f) Test of significance of  $\alpha_4$ .

Table 5: Summary results of the HAV surveillance data analysis.

THBM-I	THBM-II	NPLCM	SC	QSM	PQSM	LLM	$M_{tb}$	$M_{bh}$	IM
$\hat{N}$	633	546	516	971	1313	1325	1312	587	668
CI*	(400, 1472)	(433, 694)	(337, 784)	(557, 3583)	(669, 3171)	(607, 2718)	(464, 1961)	(287, 1110)	(339, $1.95 \times 10^{11}$ )

THBM: Trivariate Heterogeneous Bernoulli Model; NPLCM: Nonparametric Latent Class Model; SC: Sample Coverage; QSM: Quasi-symmetry Model;

PQSM: Partial Quasi-symmetry Model; LLM: Log-linear Model,  $M_{tb}$ : Time and Behavioural Response Variation Model,

$M_{bh}$ : Individual Heterogeneity and Behavioural Response Variation Model, IM: LLM without interaction effects;

\* For THBM-I, THBM-II, and NPLCM, CI refers to HPD Credible Interval.

this purpose, a novel model for capture-recapture data is considered and a Bayesian methodology has been developed to estimate the population size based on data augmentation. In particular, the Gibbs sampling method has been developed to make the computation fast and implementation easy for the practitioners. The proposed method seems to have an edge in terms of ease of interpretation and to have a much wider domain of applicability in the fields of public health, demography, and social sciences. From the simulation study, we can see that the proposed method exhibits a remarkable improvement over the existing models. Moreover, the proposed method is robust with respect to model misspecification. Along with the estimate of the population size, the posterior distribution of the associated dependence parameters and capture probabilities provide specific insights into the capture-recapture mechanism. In particular, the proposed method provides a clear picture of the nature and the extent of behavioural dependence of the individuals in the population under consideration. In real applications, we exhibit the importance of geospatial analysis of outbreaks in surveillance and identification of associated risk factors. We also emphasized the necessity to adjust the conventional method of calculating PR incorporating the estimated size of the underreported cases for an unbiased evaluation of the interventions. In a frequentist setup, a possible direction for further research could be the development of an estimation methodology based on a suitable pseudo-likelihood approach. Multiple systems estimation strategies have recently been applied to estimate the number of victims of human trafficking and modern slavery. In this context, it is not uncommon to find sparse or even no overlap between some of the lists on which the estimates are based (Chan et al., 2021). It will be an interesting problem to model such data by using the TBM and to develop an associated estimation methodology.

## Acknowledgement

The authors like to thank Mr. Debjit Majumder for his help in creating the bar diagrams. The work of Dr. Prajamitra Bhuyan is supported in part by the Lloyd's Register Foundation programme on data-centric engineering at the Alan Turing Institute, UK. The work of Dr. Kiranmoy Chatterjee is funded by (Core Research Grant CRG/2019/003204) the Science and Engineering Research Board (SERB), Department of Science & Technology, Government of India at Bidhannagar College Kolkata. Both authors contributed equally to this paper.

## Supplementary Information

Supplementary material is openly available at doi:[10.13140/RG.2.2.14598.34886](https://doi.org/10.13140/RG.2.2.14598.34886).

## References

Aldrich, J. (2002). How likelihood and identification went bayesian. *International Statistical Review*, 70(1):79–98. <https://doi.org/10.2307/1403727>. 10

Bird, S. M. and King, R. (2018). Multiple systems estimation (or capture-recapture estimation) to inform public policy. *Annu Rev Stat Appl.*, 5:95–118. 1, 2

Bohning, D. and Heijden, P. V. D. (2009). Recent developments in life and social science applications of capture–recapture methods. *Advanced Statistical Analysis*, 93:1–3. <https://doi.org/10.1007/s10182-008-0097-7>. 2

Brandsema, P. S., Euser, S. M., Karagiannis, I., Den Boer, J. W., and Van Der Hoek, W. (2014). Summer increase of Legionnaires' disease 2010 in the netherlands associated with weather conditions and implications for source finding. *Epidemiology and Infection*, 142(11):2360–2371. 25, 26

Brown, C. R., MacLachlan, J. H., and Benjamin, C. C. (2017). Addressing the increasing global burden of viral hepatitis. *Hepatobiliary Surgery and Nutrition*, 6(4):274–276. 4

Centers for Disease Control and Prevention (2021). CDC surveillance classifications. <https://www.cdc.gov/legionella/health-depts/surve-reporting/surveillance-classifications.html>. 26

Chan, L., Silverman, B. W., and Vincent, K. (2021). Multiple systems estimation for sparse capture data: Inferential challenges when there are non overlapping lists. *Journal of the American Statistical Association*, 116(535):1297–1306. <https://doi.org/10.1080/01621459.2019.1708748>. 31

ChandraSekar, C. and Deming, W. E. (1949). On a method of estimating birth and death rates and the extent of registration. *Journal of the American Statistical Association*, 44:101–115. <https://doi.org/10.2307/2280353>. 2, 5

Chao, A. (2001). An overview of closed capture–recapture models. *Journal of Agricultural, Biological, and Environmental Statistics*, 6:158–175. 6

Chao, A. (2015). Capture-recapture for human populations. *Wiley StatsRef: Statistics Reference Online*, John Wiley & Sons, Ltd, page 158–175. 5, 6

Chao, A., Chu, W., and Chiu, H. H. (2000). Capture-recapture when time and behavioral response affect capture probabilities. *Biometrics*, 56:427–433. 15

Chao, A. and Tsay, P. K. (1998). A sample coverage approach to multiple-system estimation with application to census undercount. *Journal of American Statistical Association*, 93:283–293. 5, 6, 8, 10, 16

Chao, A., Tsay, P. K., Lin, S. H., Shau, W. Y., and Chao, D. Y. (2001). The application of capture-recapture models to epidemiological data. *Statistics in Medicine*, 20:3123–3157. 2, 5, 6, 10

Chao, D., Shau, W., Lu, C., Chen, K., Chu, C., Shu, H., and Horng, C. (1997). A large outbreak of hepatitis A in a college school in Taiwan: associated with contaminated food and water dissemination. *Epidemiology Bulletin, Department of Health, Executive Yuan, Taiwan Government*, page 693–702. 4, 29

Chatterjee, K. and Bhuyan, P. (2020a). On the estimation of population size from a dependent triple-record system. *Journal of Royal Statistical Society, Series A*, 182:1487–1501. [5](#), [7](#), [8](#), [10](#), [15](#)

Chatterjee, K. and Bhuyan, P. (2020b). On the estimation of population size from a post-stratified two-sample capture–recapture data under dependence. *Journal of Statistical Computation and Simulation*, 819–838. [3](#)

Chen, W. C., Chiang, P. H., Liao, Y. H., Huang, L. C., Hsieh, Y. J., Chiu, C. M., Lo, Y. C., Yang, C. H., and Yang, J. Y. (2019). Outbreak of hepatitis A virus infection in Taiwan, June 2015 to September 2017. *Euro Surveill*, Apr 4:24(14). [4](#)

Cormack, R. M. (1989). Log-linear models for capture-recapture. *Biometrics*, 45:395–413. [5](#)

Coull, B. A. and Agresti, A. (1999). The use of mixed logit models to reflect heterogeneity in capture-recapture studies. *Biometrics*, 55:294–301. [10](#)

Coumans, A. M., Cruyff, M., Heijden, P. G. M., Heijden, V. D., Wolf, J., and Schmeets, H. (2017). Estimating homelessness in the Netherlands using a capture-recapture approach. *Social Indicators Research*, 130:189–212. [5](#)

Crowcroft, N., Walsh, B., Davison, K. L., Gungabissoon, U., and PHLS Advisory Committee on Vaccination and Immunisation (2001). Guidelines for the control of hepatitis a virus infection. *Communicable Disease and Public Health*, 4(3):213–227. [29](#)

Cruyff, M., Van Dijk, J., and van der Heijden, P. G. M. (2017). The challenge of counting victims of human trafficking: Not on the record: A multiple systems estimation of the numbers of human trafficking victims in the Netherlands in 2010–2015 by year, age, gender, and type of exploitation. *Chance*, 30:41–49. [2](#)

Cuthbert, J. A. (2001). Hepatitis A: old and new. *Clin Microbiol Rev.*, 14:38–58. [4](#)

Darroch, J. N., Fienberg, S. E., Glonek, G. F. V., and Junker, B. W. (1993). A three-sample multiple-recapture approach to census population estimation with heterogeneous catchability. *Journal of the American Statistical Association*, 88:1137–1148. [5](#), [8](#), [15](#)

Den, B. J. W., Friesema, I. H. M., and Hooi, J. D. (2002a). Reported cases of Legionella pneumonia in the Netherlands, 1987-2000 [in dutch]. *Ned Tijdschr Geneeskd.*, 146:315–320. [4](#)

Den, B. J. W., Yzerman, E. P. F., Schellekens, J., Lettinga, K. D., Boshuizen, H. C., Van Steenbergen, J. E., Bosman, A., Van den Hof, S., Van Vliet, H. A., Peeters, M. F., Van Ketel, R. J., Speelman, P., Kool, J. L., , and Van Spaendonck, M. A. E. C. V. (2002b). A large outbreak of Legionnaires' disease at a flower show, the Netherlands, 1999. *Emerg Infect Dis.*, 8:37–43. [3](#)

Dey, R. and Ashbolt, N. J. (2020). Legionella infection during and after the COVID-19 pandemic. *ACS ES&T Water*, acsestwater.0c00151. [3](#)

Farnham, A., Alleyne, L., Cimini, D., and Balter, S. (2014). Legionnaires' disease incidence and risk factors, new york, new york, usa, 2002-2011. *Emerging Infectious Diseases*, 20(11):1795–1802. [26](#)

Fienberg, S. E. (1972). The multiple recapture census for closed populations and incomplete  $2^k$  contingency tables. *Biometrika*, 59:591–603. [5](#), [15](#), [16](#)

Fischer, M. J. (2000). The folded EGB2 distribution and its application to financial return data. *Discussion Papers 32/2000*, pages Friedrich–Alexander University Erlangen–Nuremberg, Chair of Statistics and Econometrics. [13](#)

Gallay, A., Vaillant, V., Bouvet, P., Grimont, P., and Desenclos, J. (2000). How many food-borne outbreaks of Salmonella infection occurred in France in 1995? Application of the capture–recapture method to three surveillance systems. *Am. J. Epidemiol.*, 152:171–177. [2](#)

Geweke, J. (1992). Evaluating the accuracy of sampling-based approaches to the calculation of posterior moments. *J.M. Bernardo, J.O. Berger, A.P. Dawid and A.F.M. Smith (eds.), Bayesian Statistics, Oxford University Press, Oxford*, 4:169–193. [17](#), [24](#)

Goodman, L. A. (1974). Exploratory latent structure analysis using both identifiable and unidentifiable models. *Biometrika*, 61:215–231. [5](#)

Gustafson, P. (2005). On model expansion, model contraction, identifiability and prior information: Two illustrative scenarios involving mismeasured variables. *Statistical Science*, 20(1):111–140. [10](#), [11](#)

Hook, E. B. and Regal, R. (1995). Capture–recapture methods in epidemiology: methods and limitations. *Epidemiol. Rev.*, 17:243–264. [2](#)

International Working Group for Disease Monitoring and Forecasting (1995). Capture–recapture and multiple-record systems estimation I: History and theoretical development. *American Journal of Epidemiology*, 142:1047–1058. [2](#), [5](#), [6](#)

Islam, H. W. (2015). *Estimating the Missing People in the UK 1991 Population Census*. AuthorHouse, UK. [24](#)

Johnson, N. L., Kotz, S., and Balakrishnan, N. (1994). *Continuous Univariate Distributions, Band 1*. John Wiley & Sons, New York-Chichester-Brisbane, 2nd edition. [13](#)

Kadane, J. B., Meyer, M. M., and Tukey, J. W. (1999). Yule’s association paradox and ignored stratum heterogeneity in capture-recapture studies. *Journal of the American Statistical Association*, 94:855–859. [24](#)

Karagiannis, I., Brandsema, P., and Van Der Sande, M. (2009). Warm, wet weather associated with increased Legionnaires’ disease incidence in the netherlands. *Epidemiology and Infection*, 137:181–187. [25](#), [26](#)

Lai, C. C., Wang, C. Y., and Hsueh, P. R. (2020). Co-infections among patients with COVID-19: The need for combination therapy with non-anti-SARS-CoV-2 agents? *J. Microbiol Immunol Infect*, 53:505–512. [3](#)

Lettinga, K. D., Verbon, A., Weverling, G.-J., Schellekens, J. F. P., Boer, J. W. D., Yzerman, E. P. F., Prins, J., Boersma, W. G., van Ketel, R. J., Prins, J. M., and Speelman, P. (2002). Legionnaires’ disease at a dutch flower show: prognostic factors and impact of therapy. *Emerg Infect Dis.*, 8:1448–1454. [3](#)

Manrique-Vallier, D. (2016a). Bayesian population size estimation using dirichlet process mixtures. *Biometrics*, 72:1246–1254. [6](#)

Manrique-Vallier, D. (2016b). Bayesian population size estimation using dirichlet process mixtures. *Biometrics*, 72:1246–1254. [16](#)

Martin, A. and Lemon, S. M. (2006). Hepatitis A virus: from discovery to vaccines. *Hepatology*. [4](#)

Matin, N., Grant, A., Granerod, J., and Crowcroft, N. (2006). Hepatitis a surveillance in england – how many cases are not reported and does it really matter? *Epidemiology and Infection*, 134:1299–1302. [29](#)

Nardone, A., Decladt, B., Jarraud, S., Etienne, J., Hubert, B., Infuso, A., Gallay, A., and Desenclos, J. C. (2003). Repeat capture–recapture studies as part of the evaluation of the surveillance of Legionnaires’ disease in France. *Epidemiol Infect.*, 131:647–654. [4](#)

O’Hara, R. B., Lampila, S., and Orell, M. (2009). Estimation of rates of births, deaths, and immigration from mark-recapture data. *Biometrics*, (65):275–281. [2](#)

Otis, D. L., Burnham, K. P., White, G. C., and Anderson, D. R. (1978). Statistical inference from capture data on closed animal populations. *Wildlife Monographs: A Publication of Wildlife Society*, (62):3–135. [5](#), [6](#), [9](#)

Papoz, L., Balkau, B., and Lelleouch, J. (1996). Case counting in epidemiology: Limitations of methods based on multiple data sources. *International Journal of Epidemiology*, 25:474–478. [2](#)

Passer, J. K., Danila, R. N., Laine, E. S., Como-Sabetti, K. J., Tang, W., and Searle, K. M. (2020). The association between sporadic Legionnaires’ disease and weather and environmental factors, minnesota, 2011–2018. *Epidemiology and Infection*. [26](#)

Rivest, L.-P. and Baillargion, S. (2022). Loglinear models for capture-recapture experiments. *CRAN*. Date of publication: 2022-05-04. [5](#)

Rivest, L.-P. and Levesque, T. (2001). Improved log-linear model estimators of abundance in capture-recapture experiments. *The Canadian Journal of Statistics*, 29:555–572. [16](#)

Ruche, G. L., Dejour-Salamanca, D., Bernillon, O. P., Leparc-Goffart, I., Ledrans, M., Armengaud, A., Debruyne, M., Denoyel, G.-A., Brichler, S., Ninove, L., Després, P., and Gastellu-Etchegorry, M. (2013). Capture–recapture method for estimating annual incidence of imported dengue, France, 2007–2010. *Emerging Infectious Diseases*, 19:1740–1748. [2](#), [10](#)

Sanathanan, L. (1972a). Estimating the size of a multinomial population. *The Annals of Mathematical Statistics*, 43:142–152. [9](#)

Sanathanan, L. (1972b). Models and estimation methods in visual scanning experiments. *Technometrics*, 43:813–829. [5](#)

Tanner, M. A. and Wong, W. H. (1987). The calculation of posterior distributions by data augmentation. *Journal of the American Statistical Association*, 82:528–540. [11](#), [13](#)

Tsay, P. K. and Chao, A. (2001). Population size estimation for capture-recapture models with applications to epidemiological data. *Journal of Applied Statistics*, 28:25–36. [4](#), [6](#), [10](#)

Tsou, T., Liu, C., Huang, J., Tsai, K., and Chang, H. (2011). Change in hepatitis a epidemiology after vaccinating high risk children in taiwan, 1995–2008. *Vaccine*, 29(16):2956–2961. [29](#)

Van Hest, N. A. H., Hoebe, C. J. P. A., Den Boer, J. W., Vermunt, J. K., Ijzerman, E. P. F., Boersma, W. G., and Richardus, J. H. (2008). Incidence and completeness of notification of Legionnaires' disease in the Netherlands: covariate capture–recapture analysis acknowledging regional differences. *Epidemiol Infect*, 136:540–550. [3](#), [4](#), [6](#)

Van Hest, R. (2007). *Capture-recapture methods in surveillance of Tuberculosis and other infectious diseases*. Print Partners Ipskamp, Enschede. [2](#)

Wechsler, S., Izbicki, R., and Esteves, L. G. (2013). A bayesian look at nonidentifiability: A simple example. *The American Statistician*, 67(2):1537–2731. [11](#)

White, H. (1982). Maximum likelihood estimation of misspecified models. *Econometrica*, 50:1–25. [10](#)

Wolter, K. M. (1986). Some coverage error models for census data. *Journal of the American Statistical Association*, 81:338–346. [24](#)

World Health Organization (2021). WHO Hepatitis A - Diagnosis. <https://www.who.int/news-room/fact-sheets/detail/hepatitis-a>. 28

Zaslavsky, A. M. and Wolfgang, G. S. (1993). Triple-system modeling of census, post-enumeration survey, and administrative-list data. *Journal of Business and Economic Statistics*, 11:279–288. 2, 3

Zhou, F., Yu, T., Du, R., Fan, G., Liu, Y., Liu, Z., Xiang, J., Wang, Y., Song, B., Gu, X., Guan, L., Wei, Y., Li, H., Wu, X., Xu, J., Tu, S., Zhang, Y., Chen, H., and Cao, B. (2020). Clinical course and risk factors for mortality of adult inpatients with COVID-19 in Wuhan, China: A retrospective cohort study. *Lancet*, 395:1054–1062. 3